Am J Transl Res 2023;15(4):2304-2328
www.ajtr.org /ISSN:1943-8141/AJTR0148687

Original Article

Glucose 6 phosphatase dehydrogenase (G6PD): a novel diagnosis marker related to gastrointestinal cancers

Pin Zheng*, Han-He Pan*, Xi-Han Zhou, Yi-Ying Qiu, Jing Hu, Zong-Shuai Qin, Tong-Hua Wang

*Department of Gastroenterology, The Affiliated Hospital of Youjiang Medical University for Nationalities, Baise 533000, Guangxi, China. *Equal contributors.*

Received December 22, 2022; Accepted March 10, 2023; Epub April 15, 2023; Published April 30, 2023

Abstract: Background: Glucose 6 phosphatase dehydrogenase (G6PD) is a key regulator of the pentose phosphate pathway (PPP). However, the exact role of G6PD in gastrointestinal cancers remains unclear. The purpose of this study is to explore the correlation of G6PD with clinical features, pathological stages, diagnosis and prognosis of gastrointestinal cancers, as well as uncover possible mechanisms of G6PD on mutations, immunity and signaling pathways. Methods: G6PD mRNA expression data were downloaded from TCGA and GEO databases. Protein expression was examined by the HPA database. The correlation of G6PD expression with clinical and pathological characteristics was explored. The pROC package in R language was used to evaluate the diagnostic value of G6PD expression in gastrointestinal cancers. We accessed the correlation of disease-free survival (DFS) with G6PD online by Kaplan-Meier plotter. Univariate Cox regression and stepwise multiple Cox regression analysis were performed to determine the association between G6PD and patient's overall survival. In addition, genomic alterations, mutation profiles, immune infiltration, drug sensitivity and enrichment analysis related with G6PD were visualized. Results: After a pan-cancerous genomic analysis, we found that G6PD expression was the highest in African American esophageal carcinoma (ESCA) patients (P<0.05). G6PD was correlated with age, weight, disease stage, lymph node metastasis and pathological grade. Notably, G6PD showed an excellent predictive diagnosis ability for liver hepatocellular carcinoma (LIHC) (AUC=0.949, 95% CI=0.925-0.973, P<0.001). G6PD can improve the DFS of esophageal adenocarcinoma (EAC) and pancreatic adenocarcinoma (PAAD) patients (P<0.05). Both Univariate Cox regression and stepwise multiple Cox regression analysis in R language determined that G6PD expression was closely related with LIHC (P<0.001). G6PD was found to have a high mutation rate in colon adenocarcinoma and ESCA and gene amplification in ESCA, Cholangiocarcinoma, PAAD and LIHC. Copy number of G6PD was missing in LIHC. G6PD was also related to mutation of TP53 (P<0.05). Particularly, it was positively correlated with CD276 in all gastrointestinal cancers and negatively with HERV-H LTR-associating 2 in ESCA and stomach adenocarcinoma. The abnormal expression of G6PD was related to the increase of CD4+ Th2 subsets and the decrease of CD4+ (non-regulatory) of T cells. G6PD was sensitive to FK866, Phenformin, AICAR etc., while resistant to RO-3306, CGP-082996, TGX221 etc. G6PD was found to closely interact with TALDO1, GAPDH and TP53. G6PD related biological processes included aging, nutritional response and daunorubicin metabolism, and related pathways included PPP, cytochrome P450 metabolism of exogenous substances and glutathione metabolism. Conclusion: G6PD is highly expressed in gastrointestinal cancers. It is a carcinogenic indicator related to prognosis and can be used as a potential diagnostic marker of gastrointestinal cancers, so as to provide new strategy for cancer treatment.

Keywords: Gastrointestinal cancers, G6PD, diagnostic marker, prognosis

Introduction

In recent years, the incidence and mortality of cancers have been rising, and cancers have become the main cause of human death [1]. Gastrointestinal cancers include esophageal carcinoma (ESCA), stomach adenocarcinoma (STAD), liver hepatocellular carcinoma (LIHC), colon adenocarcinoma (COAD), cholangiocarcinoma (CHOL), rectum adenocarcinoma (READ) and pancreatic adenocarcinoma (PAAD). According to cancer statistics: In 2023, 1,958,310 new cancer cases and 609,820 cancer deaths are projected to occur in the United States, and gastrointestinal cancer will be an obvious cause of these deaths [2]. Among these subtypes, COAD is the most deadly, PAAD rankes second, followed by ESCA, LIHC and STAD. At present,

surgical treatment is still the main treatment for gastrointestinal cancers, but the overall success rate is still low [3]. Therefore, it's urgent to clarify the molecular pathogenesis mechanism of gastrointestinal cancers and find biomarkers for early diagnosis and treatment [4].

The Human Genome Project obtained complete human genome information in 2003 with 2.85 billion nucleotides, while the number of protein coding genes were only around 25,000 [5]. Next generation sequencing is an accurate genome sequencing tool [6]. Genomics projects such as the Cancer Genome Atlas (TCGA) and Gene Expression Omnibus (GEO) provide not only molecular expression data, but also clinical data, allowing researchers to analyze the impact of a single gene or multiple genes on cancer prognosis.

Glucose 6 phosphatase dehydrogenase (G6PD) is an important rate limiting enzyme of the pentose phosphate pathway (PPP) [7, 8]. G6PD is located in the cytoplasm of red blood cells and prevents oxidative damage [9]. PPP can produce nicotinamide adenine dinucleotide phosphate (NADPH) and ribose 5-phosphate, which play a major role in cell synthesis, such as helping fatty acid synthesis [10, 11]. PPP can also reduce glutathione, enhance antioxidant capacity and contribute to cell proliferation [12]. However, patients with G6PD deficiency suffer from a variety of diseases, including infection, neonatal jaundice, drug hemolysis, erythrocytic hemolytic anemia, etc. [13, 14].

It has been reported that the expression of G6PD in cancer cells is higher than that in normal cells, and G6PD is closely related to the overall survival rate of patients [12, 15]. P53 has been proved to be related to tumor formation, and can bind to G6PD to block the formation of active dimers. Relevant reports have also shown that p53 mutation inhibited G6PD activity [16]. The increase of G6PD promoted the proliferation of various types of cancers, including STAD [17], LIHC [18, 19], glioma [20], COAD [21] and ESCA [22].

At present, systematic studies on G6PD in gastrointestinal cancers are still needed to provide a comprehensive understanding of gastrointestinal cancers. So we conducted a variety of bioinformatics analyses, such as evaluation of differentially expressed mRNA (DEMs), Kaplan-Meier (KM) maps and gene set enrichment analysis (GSEA) to explore the effect and mechanism of G6PD in gastrointestinal cancers.

Materials and methods

Data acquisition and processing

As a milestone cancer genomics project, TCGA has performed molecular characterization on more than 20,000 primary cancers and normal tissues corresponding to 33 cancers [23, 24]. We downloaded RNA seq data and clinical data of TCGA from the Genomic Data Commons Data Portal (https://portal.gdc.cancer.gov/) and datasets from GEO database (https://www.ncbi.nlm.nih.gov/gds) as data supplement.

Analysis of G6PD expression profiles

To examine the mRNA expression of G6PD in human normal cells, we analyzed various non-tumor tissues and single cell types based on the BioGPS database. Then, we studied G6PD mRNA expression in gastrointestinal carcinomas. The transcription level of G6PD in different cancers was analyzed using the "Gene_DE" module in the TIMER2.0 database. In the "Single Gene Analysis" module of GEPIA2, we performed DEMs analysis of non-tumor and tumor samples and evaluated the pathological staging. The threshold values were set at a *P* cut-off value of 0.05 and a log2FC cut-off value of 1, with the option "Match TCGA normal value and GTEx data" selected. Log2 (TPM+1) data were used for logarithmic scaling. Protein expression of G6PD in gastrointestinal cancers were examined using HPA database (https://www.proteinatlas.org/). All statistical significance was set at $P<0.05$.

G6PD expression with clinical features in gastrointestinal cancers

UALCAN (The University of ALabama at Birmingham CANCER data analysis Portal) (http://ualcan.path.uab.edu/) was used for data processing and visualization online. We investigated data in the database of UALCAN to evaluate the correlation between the G6PD level and the clinical features of gastrointestinal cancers (race, sex, age and weight).

G6PD expression with pathological characteristic of gastrointestinal cancers

To define the relationship between G6PD level and pathological characteristics of gastrointestinal cancers, we analyzed the data in the UALCAN database and evaluated the correlation of G6PD level with stage, grade, N, cancer histological subtypes, and cancer histology. The correlation between G6PD level and stage of gastrointestinal cancers was verified in TISDB database.

Diagnostic performance of G6PD in gastrointestinal cancers

Using the data of G6PD expression in gastrointestinal cancers and adjacent tissues from the TCGA database, we drew receiver operating characteristic (ROC) curve with R language pROC package to evaluate the diagnostic value of G6PD level in gastrointestinal cancers.

Prognostic analysis of G6PD in gastrointestinal cancers

The correlation between disease-free survival (DFS) and G6PD was accessed online using the KM plotter (http://kmplot.com/analysis/), and the KM curves were visualized to analyze the prognosis of gastrointestinal cancers. Univariate Cox regression and stepwise multiple Cox regression analysis in R language were performed to determine the association between the G6PD level and patient's overall survival.

Correlation between G6PD and gene mutation

cBioPortal (http://www.cbioportal.org/) was employed to analyze the genomic changes of G6PD in various types of cancers from TCGA. These changes included copy number amplification, deletions, missense mutations with uncertain significance, and mRNA upregulation. We compared G6PD expression in gastrointestinal cancers with different TP53 mutation status in the UALCAN database. The correlation of G6PD expression with Tumor Burden (TMB) and Microsatellite Instability (MSI) was visualized on an online platform (www.aclbi.com), which integrated samples from TCGA, GEO and other public databases.

Immune infiltration analysis

By applying the ESTIMATE algorithm, we were able to estimate the proportion of immune cells and stromal cells in tumor samples based on gene expression characteristics [25]. Using the "estimate" package in RSstudio, we calculated the ImmuneScore and StromalScore for each TCGA sample. The associations between G6PD expression and these scores were then illustrated with scatter plots, where a higher score indicates a greater infiltration of immune or matrix components in the tumor microenvironment (TME) [26].

To explore the correlation between G6PD expression and immune checkpoint-related genes in human cancers within the TCGA cohort, we utilized the "Gene_Corr" module in the TIMER2.0 database. This allowed us to generate a heat map indicating the statistical significance with ρ value after purity adjustment via Spearman's correlation analysis. Genes of interest included BTLA, CD27, CD274, CD276 and others [27]. Moreover, we employed the "immune gene" tool in TIMER2.0 to investigate the link between G6PD level and immune cell infiltration in all TCGA cancers. Specifically, we focused on Th1 and Th2 subsets of myeloid-derived suppressor cells (MDSCs) and CD4+ T cells. Using TIDE and XCELL algorithms, we estimated the immune infiltration and depicted the results with heat maps and scatter plots.

Drug sensitivity analysis

GSCALite database (http://bioinfo.life.hust.edu.cn/web/GSCALite/) integrated 265 small molecules from Genomics of Drug Sensitivity in Cancer. We searched G6PD related gene set including "immune genes" BTLA, CD27, CD274 and CD276 to perform drug sensitivity analysis. The expression of G6PD in the gene sets were explored by Spearman correlation analysis with the small molecule/drug sensitivity (IC50).

Enrichment analysis

The STRING database was used to establish a protein protein interaction (PPI) network with its default parameters [28]. The result file was imported into the Cytoscape software (version 3.9.1) to visualize the PPI network [29]. The GEPIA2 database (TCGA and GTEx data sets) was used to obtain G6PD related genes (the first 100). The TIMER2.0 database was utilized to generate a heat map of the genes related to G6PD expression. The Venn diagram tool (http://bioinformatics.psb.ugent.be/webtools/

Venn/) was used to analyze the cross genes associated with G6PD. Additionally, the DAVID database (https://david.ncifcrf.gov/) was used to analyze the function of G6PD, the CancerSEA database (http://biocc.hrbmu.edu.cn/CancerSEA/) was used to map the state of single cell function [30]. Further GSEA was conducted to analyze different signal pathways of G6PD low expression and high expression. The ES scores were sorted to show the signal path with the best ES score. The network diagrams of different cancer signal pathways were visualized by using Cytoscape.

Results

G6PD expression profiles in human normal tissues and cancers

We used the BioGPS database to study the expression of G6PD in normal tissue cells. In a variety of tissues and cells, the highest expression of G6PD was observed in whole blood, followed by CD56+ NK cells. With regard to cancer cell lines, G6PD expression was enriched in A549.1 cells (**Figure 1A**) and decreased in HELA.1 cells (**Figure 1B**).

We analyzed the expression of G6PD in cancer through TIMER2.0 database. As demonstrated in **Figure 1C**, G6PD showed a high expression level in various cancers, including bladder urothelial carcinoma, breast invasive carcinoma (BRCA), cervical squamous cell carcinoma, endocervical adenocarcinoma, CHOL, COAD, ESCA, head and neck squamous cell carcinoma (HNSC), kidney chromophobe (KICH), kidney renal papillary cell carcinoma, LIHC, lung adenocarcinoma, lung squamous cell carcinoma (LUSC), rectum adenocarcinoma (READ), STAD and uterine corpus endometrial carcinoma. Additionally, there was a significant reduction in G6PD expression in thyroid carcinoma (THCA) compared to normal samples, and also a significant decrease in G6PD expression in HPV+ HNSC cells compared to HPV- HNSC cells.

By analyzing the data of GEPIA2 database, we further analyzed the differential expression of G6PD between CHOL, COAD, ESCA, LIHC, PAAD, READ and STAD tumor tissues and normal tissues (**Figure 1D**). As showed in **Figure 1E**, G6PD had a high protein expression in COAD, LIHC and PAAD, and a medium expression in STAD.

Correlation of G6PD expression with clinical features in gastrointestinal cancers

We analyzed the correlation between G6PD expression and clinical characteristics of gastrointestinal cancer patients using the UALCAN database. As shown in **Figure 2A**, the data included 3 races: Caucasian, African American and Asian. Significant difference presented in the levels of G6PD when Normal samples vs. Tumor samples from other races respectively in COAD, LIHC and STAD; when Normal sample vs. Caucasian tumor samples, Caucasian tumor samples vs. Asian tumor samples in CHOL; when Normal samples vs. African American tumor samples or Asian tumor samples, Caucasian tumor samples vs. Asian tumor samples in ESCA; when Normal samples vs. Caucasian tumor samples or African American tumor samples in READ ($P<0.05$). G6PD showed significant difference when Normal vs. Male or Female respectively in CHOL, COAD, LIHC, READ and STAD, when Normal vs. Male in ESCA ($P<0.05$) (**Figure 2B**).

The age data were divided into 5 groups: Normal and Tumor (21-40 years, 41-60 years, 61-80 years and 81-100 years). There were significant differences in the levels of G6PD when Normal vs. other groups respectively in COAD, LIHC and READ; when Tumor (41-60 years) vs. Tumor (61-80 years) or Tumor (81-100 years), Tumor (61-80 years) vs. Tumor (81-100 years) in ESCA; when Tumor (41-60 years) vs. Tumor (61-80 years) in PAAD ($P<0.05$) (**Figure 3A**).

Weight data were also divided into 5 groups: Normal and Tumor (Normal Weight, Extreme Weight, Obese and Extreme Obese). Significant differences appeared in the levels of G6PD when Normal vs. other groups (except Extreme Obese) respectively in CHOL; when Normal vs. other groups respectively, Extreme Weight vs. Extreme Obese, Obese vs. Extreme Obese in COAD; when Normal vs. other groups respectively, Extreme Weight vs. Obese in ESCA; when Normal vs. Normal Weight or Extreme Weight in READ ($P<0.05$) (**Figure 3B**).

Correlation of G6PD expression with pathological characteristic in gastrointestinal cancers

To evaluated the correlation of G6PD expression with pathological characteristic in gastrointestinal cancers, we investigated the data

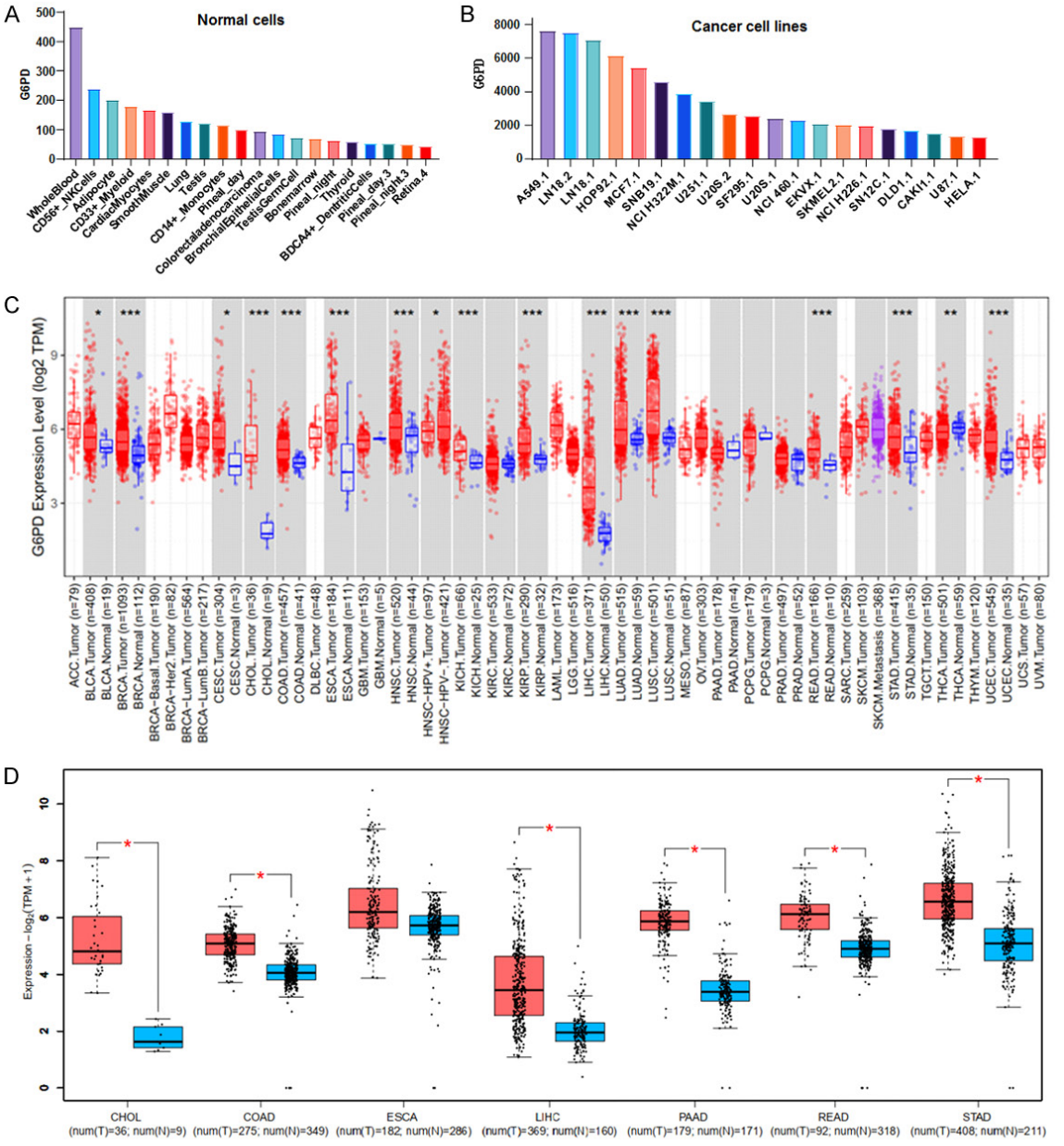

COAD	LIHC	PAAD	STAD
ID: 442	ID: 82	ID: 170	ID: 1207
Sex: Female	Sex: Female	Sex: Female	Sex: Male
Age: 78	Age: 66	Age: 52	Age: 63
Stain : High	Stain : High	Stain : High	Stain : Medium
Intensity : Strong	Intensity : Strong	Intensity : Strong	Intensity : Moderate
Quantity : > 75%	Quantity : > 75%	Quantity : > 75%	Quantity : > 75%

Figure 1. Glucose 6 phosphatase dehydrogenase (G6PD) expression profiles in normal tissues and cancers. A. G6PD expression levels in normal tissues and cell types. B. G6PD expression levels in cancer cell lines. C. Expression levels of G6PD in The Cancer Genome Atlas Program (TCGA) cancers were analyzed by TIMER 2.0 database (*P<0.05, **P<0.01, ***P<0.001). D. Differences in G6PD expression between cancers from the TCGA database and normal samples from the GEPIA2.0 database (*P<0.05). E. G6PD protein expression in Colon adenocarcinoma (COAD), Liver hepatocellular carcinoma (LIHC), Pancreatic adenocarcinoma (PAAD) and Stomach adenocarcinoma (STAD).

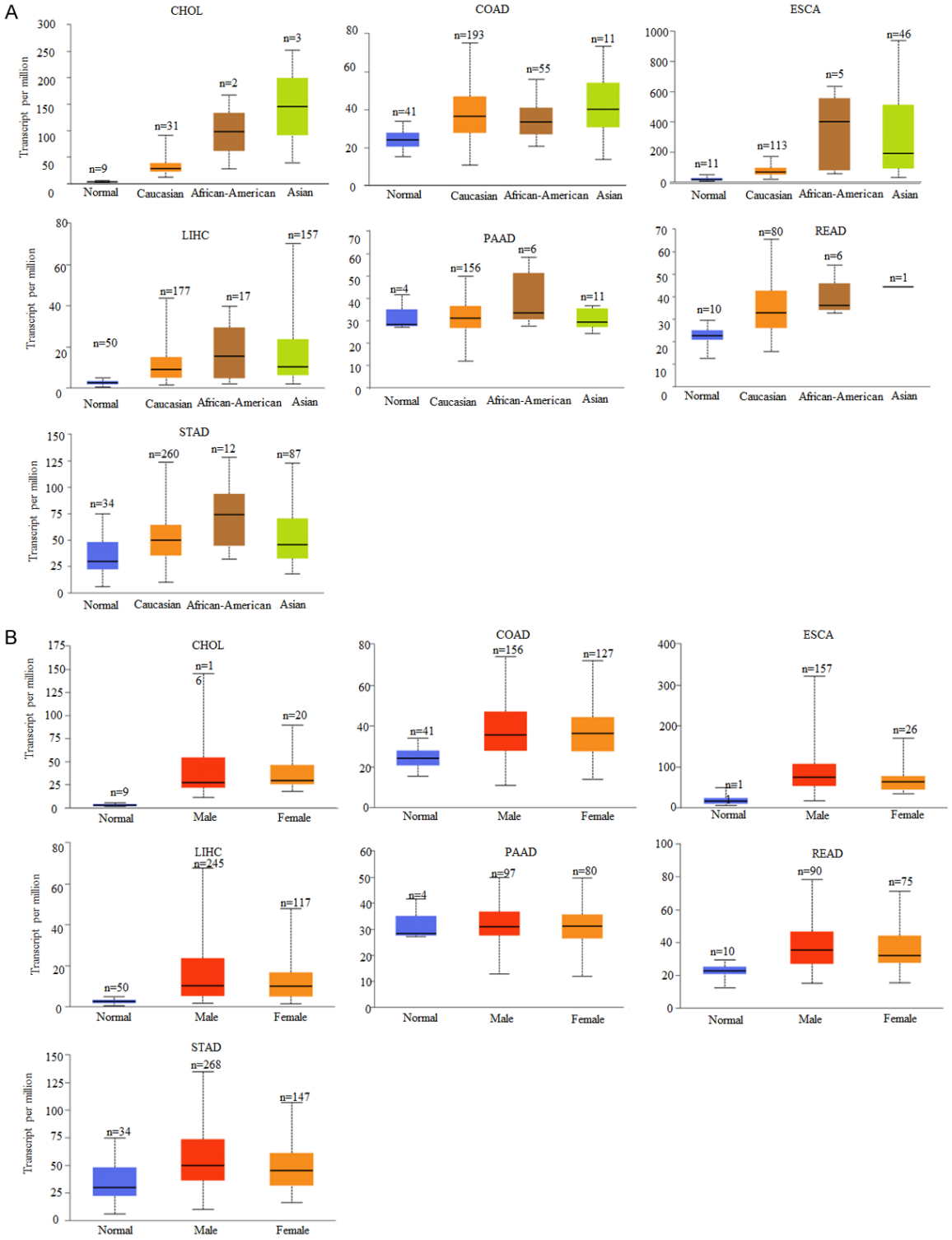

Figure 2. Glucose 6 phosphatase dehydrogenase (G6PD) expression levels in patients with different race or sex. A. G6PD expression were assessed by race (Normal, Caucasian, African American and Asian) in Cholangiocarcinoma (CHOL), Colon adenocarcinoma (COAD), Esophageal carcinoma (ESCA), Liver hepatocellular carcinoma (LIHC), Pancreatic adenocarcinoma (PAAD), Rectum adenocarcinoma (READ) and Stomach adenocarcinoma (STAD) from UALCAN database. B. G6PD expression were assessed by the sex in CHOL, COAD, ESCA, LIHC, PAAD, READ and STAD from UALCAN database.

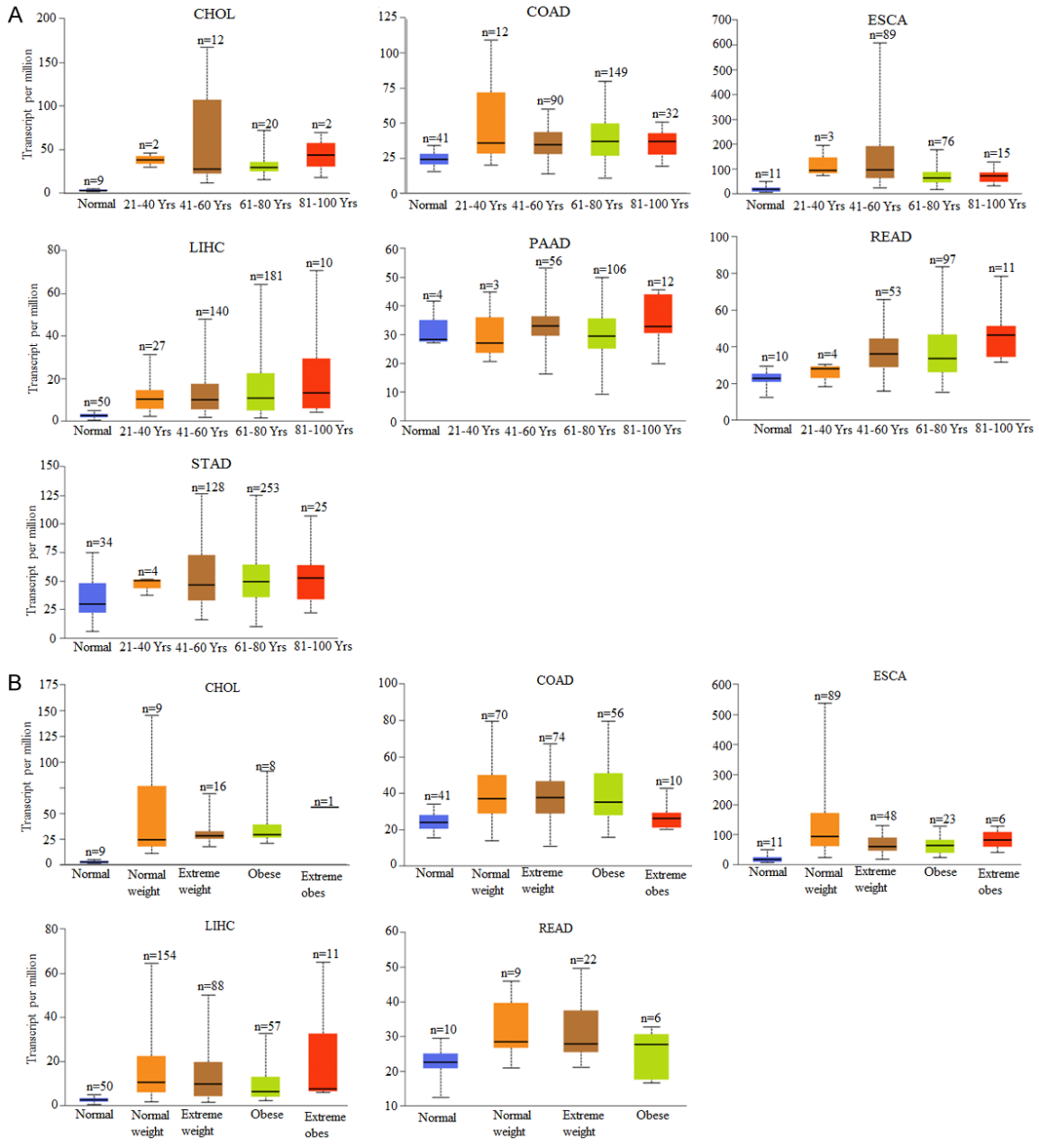

Figure 3. Glucose 6 phosphatase dehydrogenase (G6PD) expression levels in patients with different age and weight. A. G6PD expression were assessed by age in Cholangiocarcinoma (CHOL), Colon adenocarcinoma (COAD), Esophageal carcinoma (ESCA), Liver hepatocellular carcinoma (LIHC), Pancreatic adenocarcinoma (PAAD), Rectum adenocarcinoma (READ) and Stomach adenocarcinoma (STAD) from UALCAN database. B. G6PD expression were assessed by weight in CHOL, COAD, ESCA, LIHC and READ from UALCAN database.

from UALCAN database. As shown in **Figure 4**, results determined a significant difference in G6PD expression when Normal vs. Stage 1 or Stage 2 in CHOL and PAAD; when Normal vs.

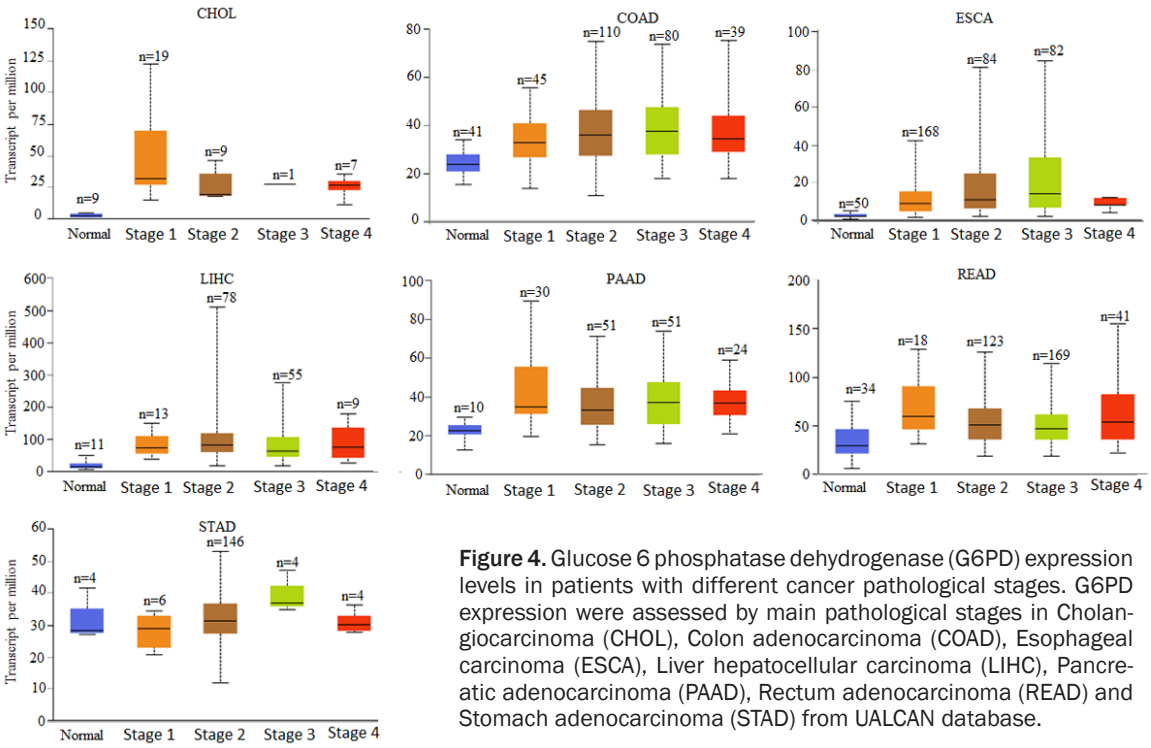

Figure 4. Glucose 6 phosphatase dehydrogenase (G6PD) expression levels in patients with different cancer pathological stages. G6PD expression were assessed by main pathological stages in Cholangiocarcinoma (CHOL), Colon adenocarcinoma (COAD), Esophageal carcinoma (ESCA), Liver hepatocellular carcinoma (LIHC), Pancreatic adenocarcinoma (PAAD), Rectum adenocarcinoma (READ) and Stomach adenocarcinoma (STAD) from UALCAN database.

Stage 2 or Stage 3, Stage 1 vs. Stage 2 in ESCA; when Normal vs. Stage 1 to Stage 4 respectively in COAD and STAD; when Normal vs. Stage 1 to Stage 4 respectively, Stage 1 vs. Stage 2 in READ (P<0.05).

Results in **Figure 5A** revealed significant difference in G6PD when Grade 2 vs. Grade 3 in ESCA; when Normal vs. Grade 1 to Grade 4 respectively, Grade 1 vs. Grade 2 or Grade 3, Grade 2 vs. Grade 3 in LIHC; when Grade 1 vs. Grade 2 or Grade 3 in PAAD; when Normal vs. Grade 2 or Grade 3, Grade 1 vs. Grade 3 in STAD (P<0.05). As shown in **Figure 5B**, G6PD expressed significant differences when Normal vs. N0 in CHOL and LIHC; when Normal vs. N0 to N2 in COAD and READ; when Normal vs. N1 or N2, N0 vs. N1 in ESCA; when Normal vs. other groups respectively in STAD (P<0.05).

For pathological stages, a significant relationship of G6PD was found when Normal vs. Adenocarcinoma or Mucinous adenocarcinoma, Adenocarcinoma vs. Mucinous adenocarcinoma in COAD and READ; when Normal or Adenocarcinoma vs. Squamous cell carcinoma in ESCA; when Normal vs. Adenocarcinoma (NOS), Intestinal Adenocarcinoma (NOS), Intestinal Adenocarcinoma (Tubular) or Intestinal Adenocarcinoma (Papillary), Adenocarcinoma (Diffuse) vs. Intestinal Adenocarcinoma (NOS) or Intestinal Adenocarcinoma (Tubular), Intestinal Adenocarcinoma (NOS) or Intestinal Adenocarcinoma (Tubular) vs. Intestinal Adenocarcinoma (Mucinous) in STAD (P<0.05) (**Figure 6A**). Moreover, G6PD expression was only significantly different in ESCA in Normal or Adenocarcinoma vs. Squamous cell carcinoma (P<0.05) (**Figure 6B**).

Diagnostic performance of G6PD in gastrointestinal cancers

ROC curves showed that G6PD expression was associated with diagnosis in cancers from TCGA database. G6PD showed an excellent predictive diagnosis ability for LIHC (AUC=0.949, 95% CI=0.925-0.973, P<0.001), COAD (AUC=0.852, 95% CI=0.814-0.889, P<0.001) and ESCA (AUC=0.807, 95% CI=0.631-0.984, P<0.001), an a good diagnosis ability for STAD (AUC=0.639, 95% CI=0.526-0.752, P<0.01). However G6PD showed no statistical significance in the diagnosis of PAAD (AUC=0.591, 95% CI=0.258-0.923, P>0.05) (**Figure 7A**).

In **Figure 7B**, G6PD didn't reveal a good predictive diagnosis ability in CHOL (AUC=0.585, 95% CI=0.480-0.690, P<0.05). Also, G6PD showed no statistical significance in the diagnosis of

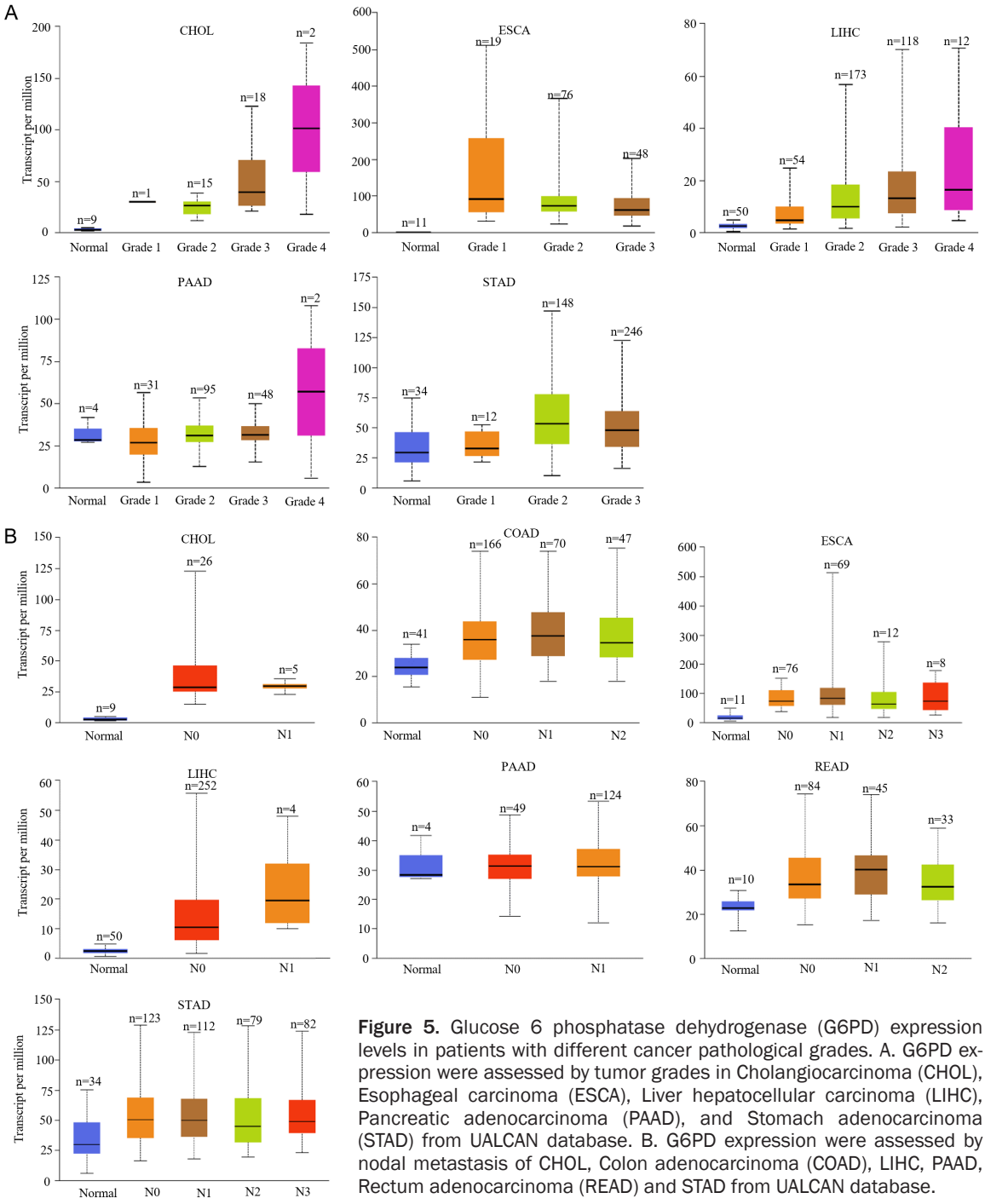

Figure 5. Glucose 6 phosphatase dehydrogenase (G6PD) expression levels in patients with different cancer pathological grades. A. G6PD expression were assessed by tumor grades in Cholangiocarcinoma (CHOL), Esophageal carcinoma (ESCA), Liver hepatocellular carcinoma (LIHC), Pancreatic adenocarcinoma (PAAD), and Stomach adenocarcinoma (STAD) from UALCAN database. B. G6PD expression were assessed by nodal metastasis of CHOL, Colon adenocarcinoma (COAD), LIHC, PAAD, Rectum adenocarcinoma (READ) and STAD from UALCAN database.

colorectal cancer (CA) (AUC=0.564, 95% CI= 0.386-0.742, *P*>0.05) and PAAD (AUC=0.632, 95% CI=0.404-0.860, *P*>0.05) based on GEO database.

Prognostic analysis of G6PD in gastrointestinal cancers

KM survival curves showed that G6PD expression was associated with prognostic outcomes in gastrointestinal cancers. **Figure 8A** shows that G6PD was associated with the DFS of gastrointestinal cancers. G6PD could improve the DFS of esophageal adenocarcinoma (EAC) (*P*<0.01) and PAAD (*P*<0.05), while conversely in LIHC (*P*<0.01) and STAD (*P*<0.05). Univariate Cox regression and stepwise multiple Cox regression analysis in R language both determined that G6PD expression was closely related with LIHC (*P*<0.001) (**Figure 8B**).

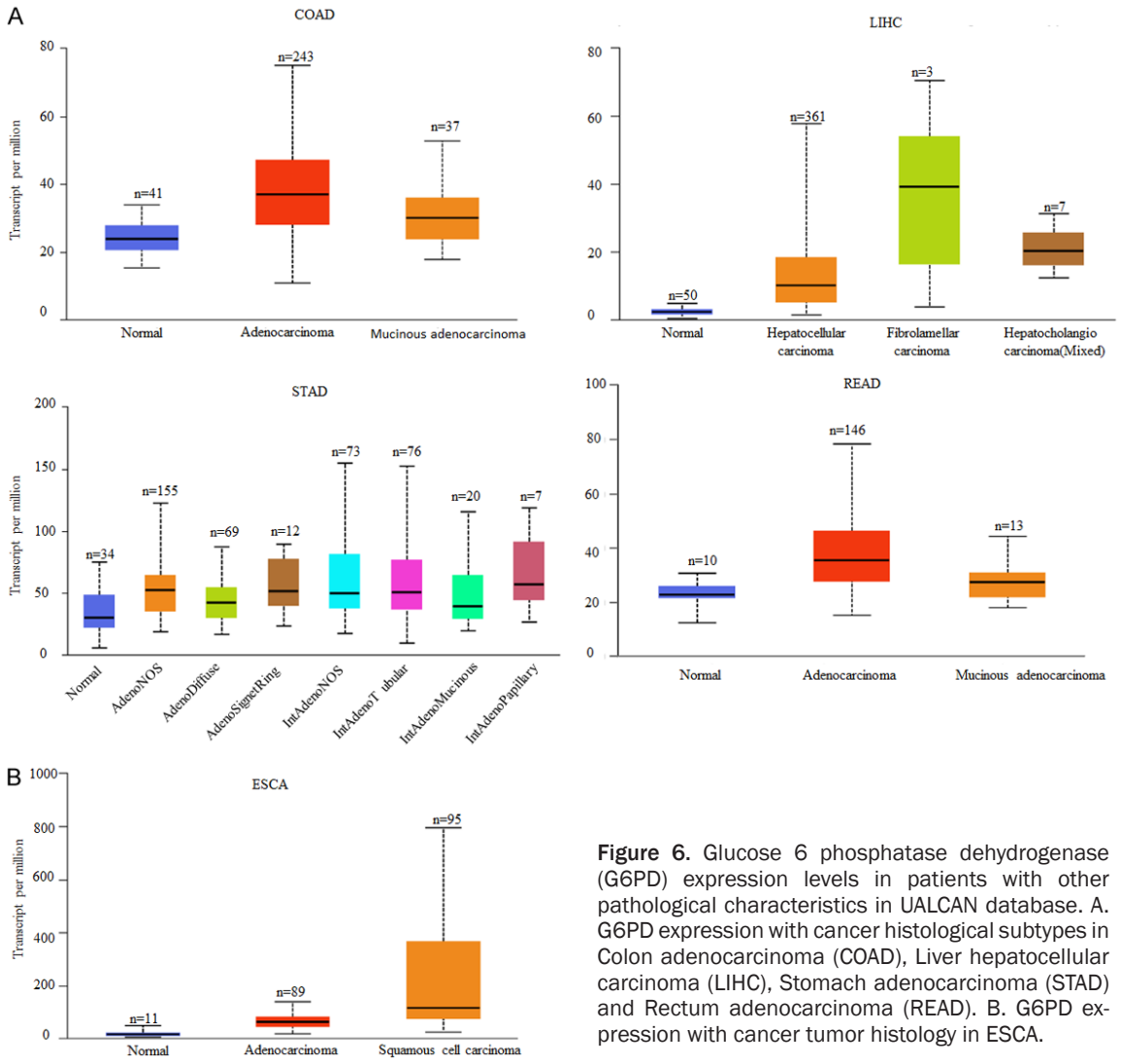

Figure 6. Glucose 6 phosphatase dehydrogenase (G6PD) expression levels in patients with other pathological characteristics in UALCAN database. A. G6PD expression with cancer histological subtypes in Colon adenocarcinoma (COAD), Liver hepatocellular carcinoma (LIHC), Stomach adenocarcinoma (STAD) and Rectum adenocarcinoma (READ). B. G6PD expression with cancer tumor histology in ESCA.

Correlation of G6PD with gene mutation

We used the cBioPortal database to examine the genomic changes and mutation profiles of G6PD in the TCGA cancer cohort. As shown in **Figure 9A**, high mutation frequency of G6PD appeared in CA and ESCA. Copy number of G6PD changed in ESCA, CHOL, PAAD and LIHC. Copy number "deep deletion" happened in LIHC. The type, site and number of cases of G6PD genome changes are shown in **Figure 9B**. The general mutation counts of G6PD in a variety of cancer samples are shown in **Figure 9C**.

In addition, we studied the relationship between G6PD expression and TP53 mutation status in UALCAN database. We found the expression of G6PD in the TP53 Mutant group was significantly higher than in the Normal and TP53 Non-Mutant group in COAD, ESCA, LIHC, PAAD, READ and STAD ($P<0.05$) (**Figure 9D**).

TMB and MSI are considered to be the key factors that affect the occurrence and development of the response of cancer immunotherapy. In **Figure 9E**, G6PD expression was positively correlated with TMB in kidney renal clear cell carcinoma (KIRC), low-grade gliomas, skin cutaneous melanoma, sarcoma, PAAD (cor= 0.159), HNSC and BRCA, while negatively in ESCA (cor=-0.311), acute myeloid leukemia and THCA cohorts ($P<0.05$). The expression of G6PD was also positively correlated with MSI in KICH, glioblastoma multiforme, KIRC and LUSC, while negatively in pheochromocytoma and paraganglioma and READ (cor=-0.251) ($P<0.05$) (**Figure 9E**).

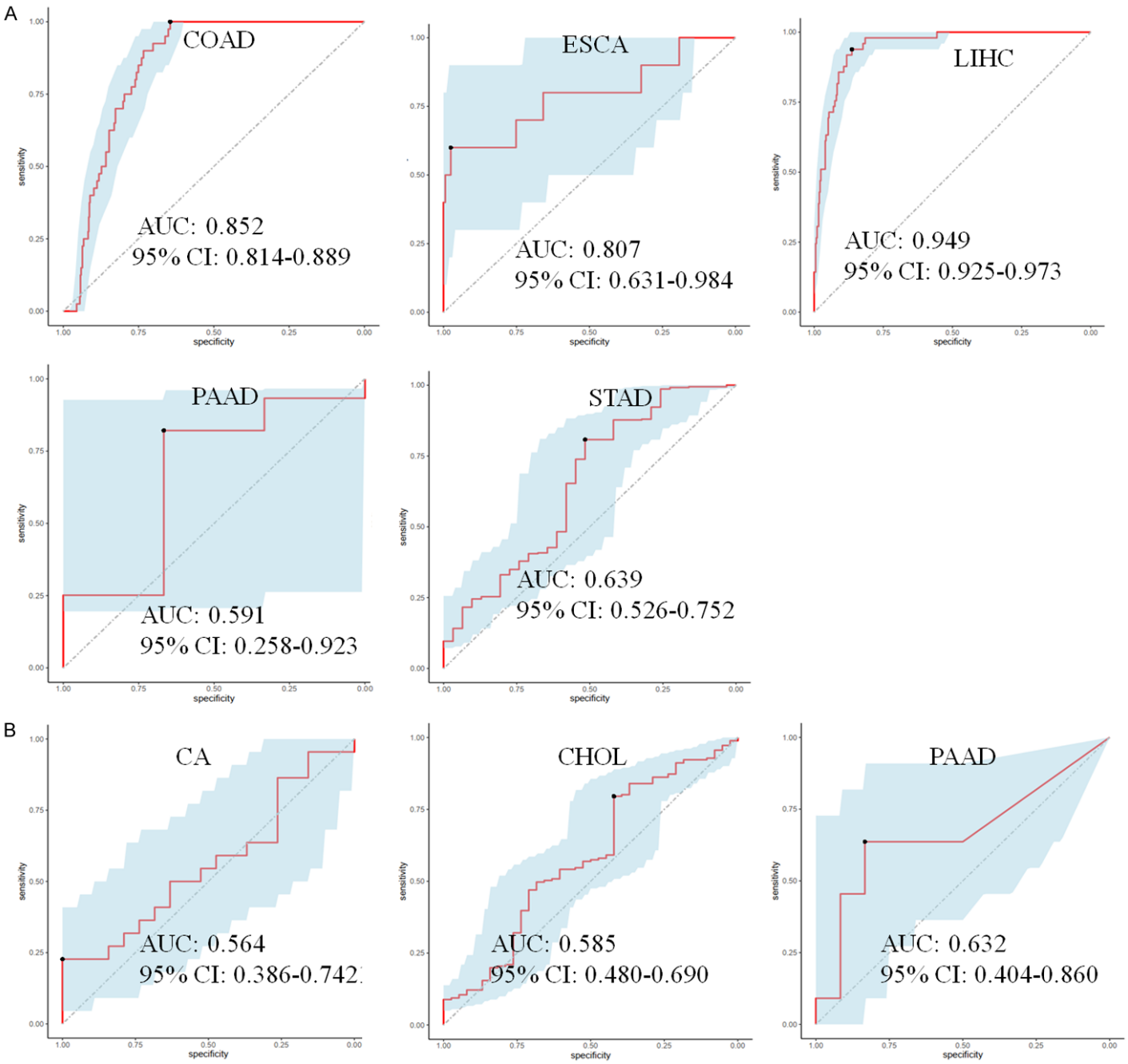
A
COAD
AUC: 0.852
95% CI: 0.814-0.889
ESCA
AUC: 0.807
95% CI: 0.631-0.984
LIHC
AUC: 0.949
95% CI: 0.925-0.973
PAAD
AUC: 0.591
95% CI: 0.258-0.923
STAD
AUC: 0.639
95% CI: 0.526-0.752
B
CA
AUC: 0.564
95% CI: 0.386-0.742
CHOL
AUC: 0.585
95% CI: 0.480-0.690
PAAD
AUC: 0.632
95% CI: 0.404-0.860
sensitivity
specificity

Figure 7. The diagnostic value of Glucose 6 phosphatase dehydrogenase (G6PD) expression level in gastrointestinal malignant tumors. A. Receiver operator characteristic (ROC) curve of G6PD expression levels in digestive tract cancer tissues and non-cancer tissues from The Cancer Genome Atlas Program (TCGA). B. ROC curve of G6PD expression levels in digestive tract tissues from Gene Expression Omnibus (GEO).

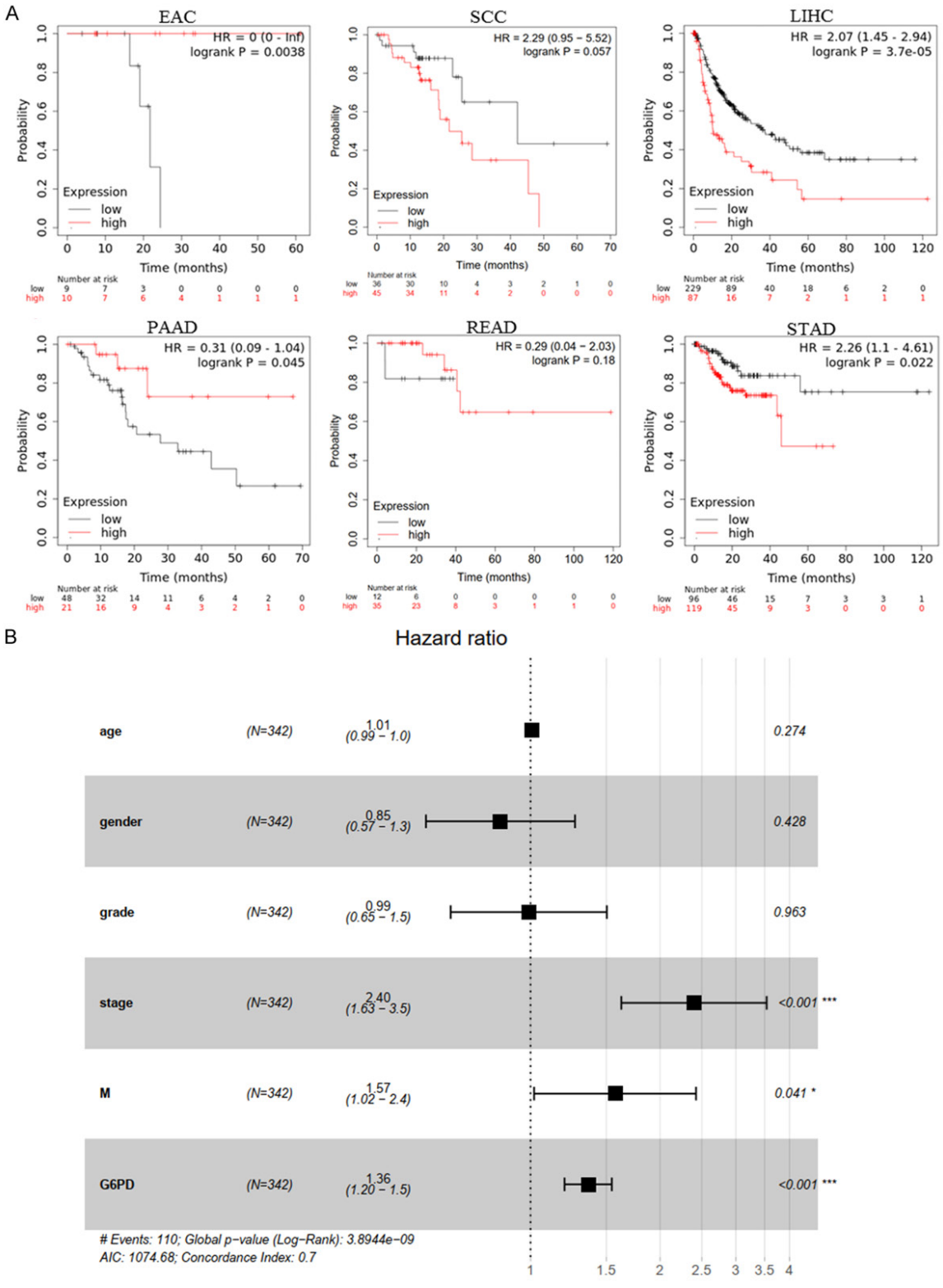

Figure 8. Prognostic Analysis of Glucose 6 phosphatase dehydrogenase (G6PD) in gastrointestinal cancers. A. G6PD expression levels related with patient's disease free survival (DFS). Correlation of G6PD expression and DFS was assessed in esophageal adenocarcinoma (EAC), Liver hepatocellular carcinoma (LIHC), Pancreatic adenocarcinoma (PAAD), Rectum adenocarcinoma (READ) and Stomach adenocarcinoma (STAD) by Kaplan-Meier Plotter. B. Multiple Cox regression analysis of G6PD expression in LIHC.

Correlation of G6PD expression with immune infiltrates in gastrointestinal cancers

We used ESTIMATE to calculate the immune and matrix scores of cancer tissues. **Figure 10A** indicated that G6PD was correlated with the immune and stromal scores in ESCA, LIHC and STAD ($P<0.05$). We found that G6PD expression was positively correlated with CD276 in all gastrointestinal cancers, while negatively with HERV-H LTR-associating 2 (HHLA2) in ESCA and STAD, as shown in **Figure 10B**. G6PD level and infiltration level of MDSCs, Th1 and Th2 subsets of T cells CD4+ across TCGA cancers Scatter plots of MDSCs are showing in **Figure 10C**. Correlation between G6PD and immune cell infiltration in all gastrointestinal cancers are showing in **Figure 10D**. G6PD expression was positively correlated with T cell CD4+ Th2_XCELL in CHOL, LIHC and READ; positively with MDSC_TIDE in CHOL, ESCA, LIHC and STAD; positively with T cell CD4+ memory activated CIBERSORT-ABS in PAAD and READ. While G6PD expression was negatively correlated with T cell CD4+ (non-regulatory) in CHOL, COAD and STAD. The profiles illustrated that G6PD was engaged in the immune infiltration-related pathways and served a critical role in the immuno-oncological interactions.

Drug sensitivity analysis

We searched G6PD related gene sets including "immune genes" BTLA, CD27, CD274, CD276 to perform drug sensitivity analysis in GSCALite database. Results showed that G6PD was sensitive to FK866, Phenformin, AICAR etc., while resistant to RO-3306, CGP-082996, TGX221 etc. (**Figure 11**).

Enrichment analysis of G6PD related genes in gastrointestinal cancers

In STRING database, a total of 47 G6PD interacting proteins were retrieved, among which PGD, HK2, LDHB, TPI1, GPI, PKM, PGLS, TALDO1, GAPDH and TP53 interacted significantly, as shown in PPI (**Figure 12A**). The first 100 genes related to G6PD expression were obtained via GEPIA2 and TIME2.0 database. The expression of G6PD was significantly positive with GMPS, TKT, ZDHHC18, NQO1, ABCC1, HK1, ME1, PGD, PRDX1, TALDO1 and USB1 (**Figure 12B**, **12C**).

We obtained 2 G6PD related genes (PGD, TALDO1) across String and GEPIA2 database (**Figure 12D**). G6PD related genes obtained from these two datasets were used for GO and KEGG enrichment analysis. As shown in **Figure 12E**, the GO function analysis showed that G6PD was related to the biological processes such as aging, nutritional response and daunorubicin metabolism. G6PD was related to molecular functions such as D-threo-aldose 1-dehydrogenase activity and oxidoreductase activity, acting on NAD(P)H and so on.

KEGG enrichment analysis showed that G6PD was related to signal pathways such as Steroid hormone biosynthesis, PPP, Metabolism of xenobiotics by cyclochrome P450, Glutathione metropolis, Ferropsis and so on (**Figure 12F**).

Single cell analysis was conducted using the Cancer SEA database. It was found that G6PD was involved in a variety of carcinogenic processes, including angiogenesis, apoptosis, cell cycle differentiation, DNA damage, etc. (**Figure 12G**).

We conducted GSEA enrichment analysis of G6PD in gastrointestinal cancers. The signal pathways with the highest ES score enriched in various cancers are shown in **Figure 13A**, including PPP (COAD/READ), ascorbic acid and aldose metabolism (ESCA), steroid biosynthesis (STAD), proteasome (PAAD), mitotic (LIHC) and mismatch repair (CHOL). We observed the correlation between G6PD and related signal pathways in various cancers through cystoscopy (**Figure 13B**). G6PD mainly acted on gastrointestinal cancer through DNA replication, mismatch repair, proteasome, homologous recombination, glutamate metabolism, PPP, RNA polymerase, base excitation repair, cell cycle porphyrin and CHOROPHYLL metabolism, py-

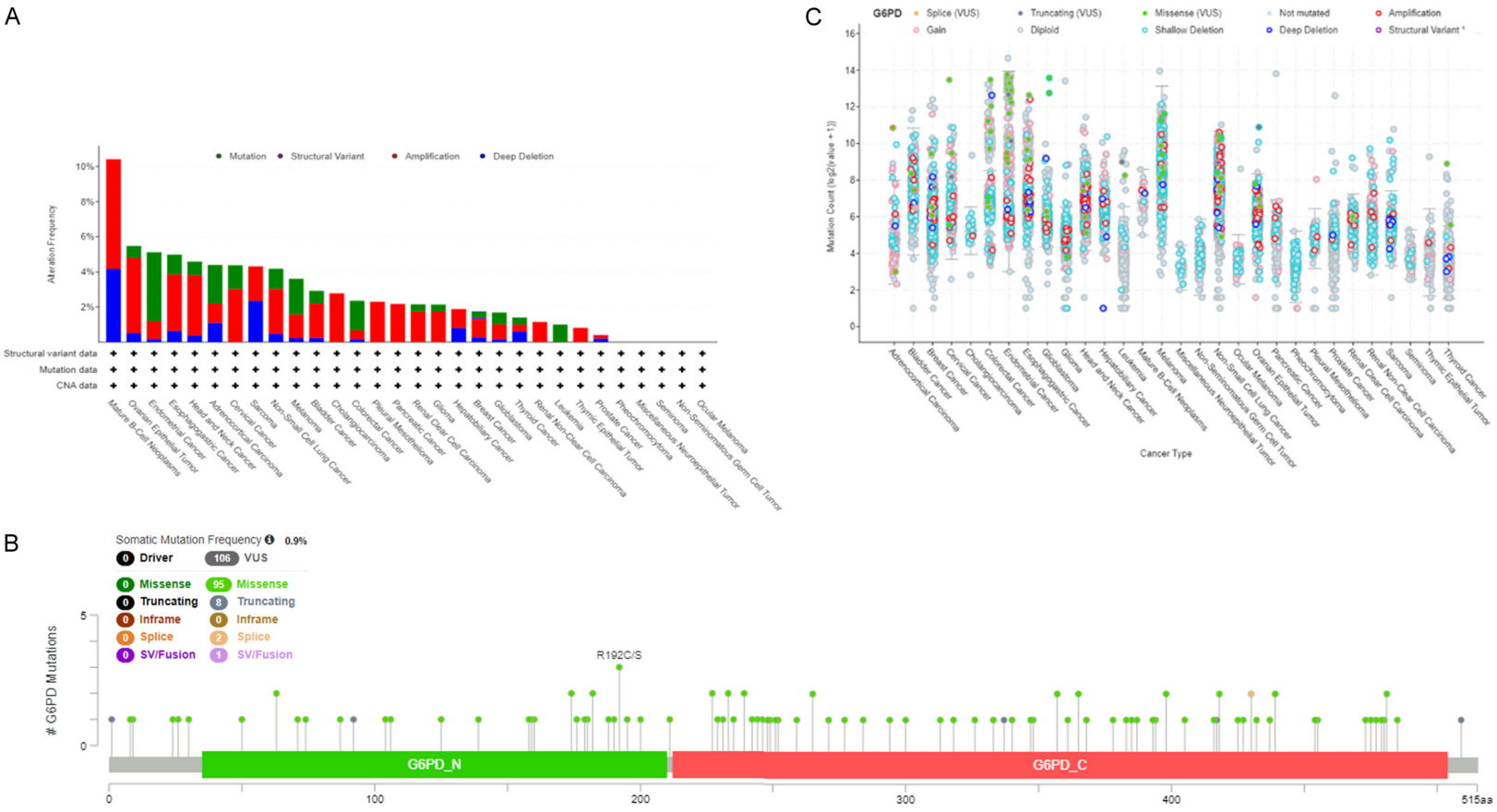
A
Mutation
Structural Variant
Amplification
Deep Deletion
Alteration Frequency
Structural variant data
Mutation data
CNA data
B
Somatic Mutation Frequency 0.9%
0 Driver
106 VUS
0 Missense
0 Truncating
0 Inframe
0 Splice
0 SV/Fusion
95 Missense
8 Truncating
0 Inframe
2 Splice
1 SV/Fusion
G6PD Mutations
R192C/S
G6PD_N
G6PD_C
0
100
200
300
400
515aa
C
G6PD
Splice (VUS)
Truncating (VUS)
Missense (VUS)
Not mutated
Amplification
Gain
Diploid
Shallow Deletion
Deep Deletion
Structural Variant
Mutation Count (log2(value + 1))
Cancer Type

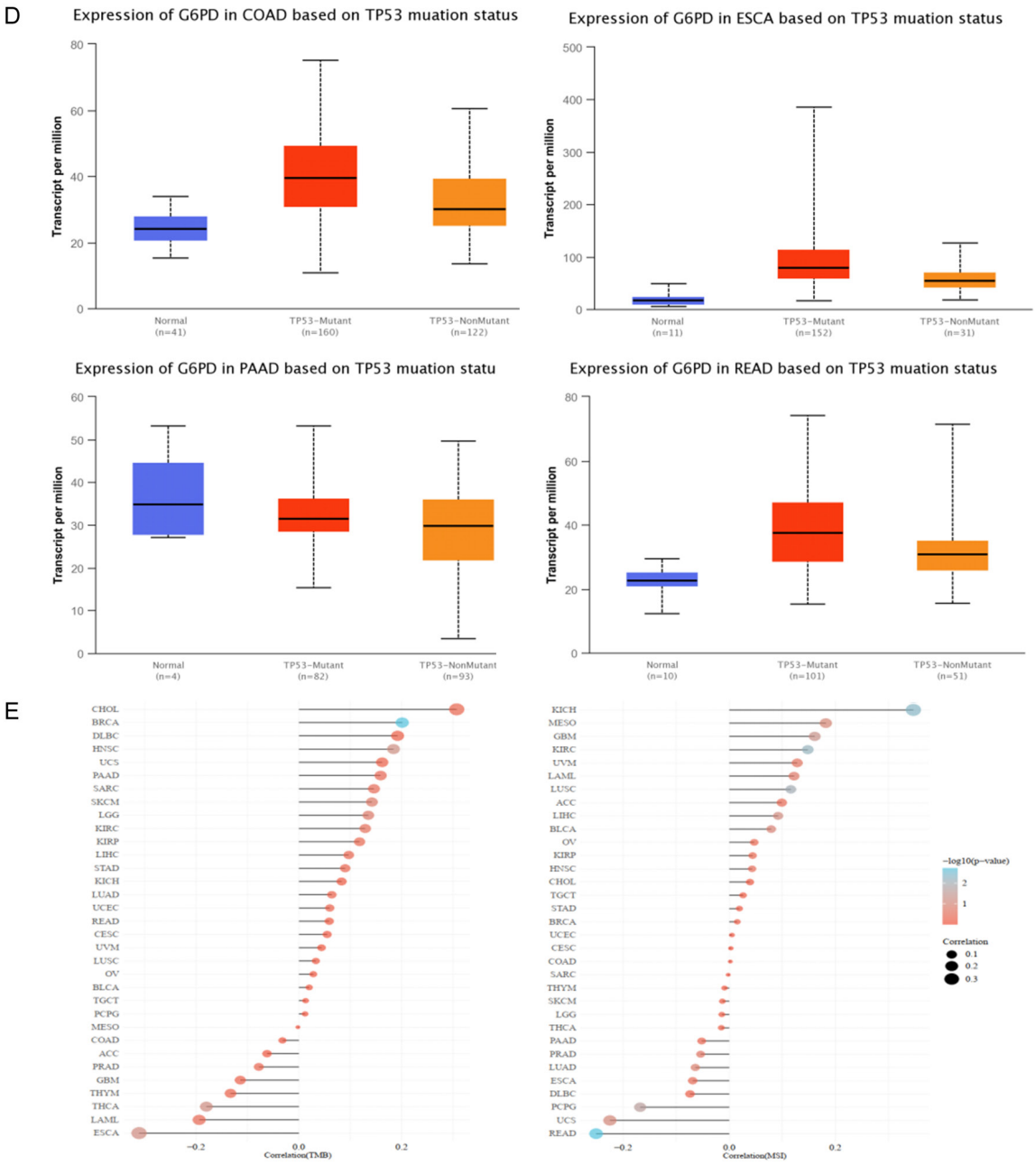

Figure 9. Mutation landscape of Glucose 6 phosphatase dehydrogenase (G6PD) in cancers. G6PD alteration frequencies in various cancers (A) and mutation sites (B) were visualized. (C) The general mutation counts of G6PD in The Cancer Genome Atlas Program (TCGA) samples. (D) Expression level of G6PD in different tumor protein p53 (TP53) mutation states in various cancers in UALCAN database. (E) Radar maps of correlations between G6PD expression and TMB and MSI were plotted.

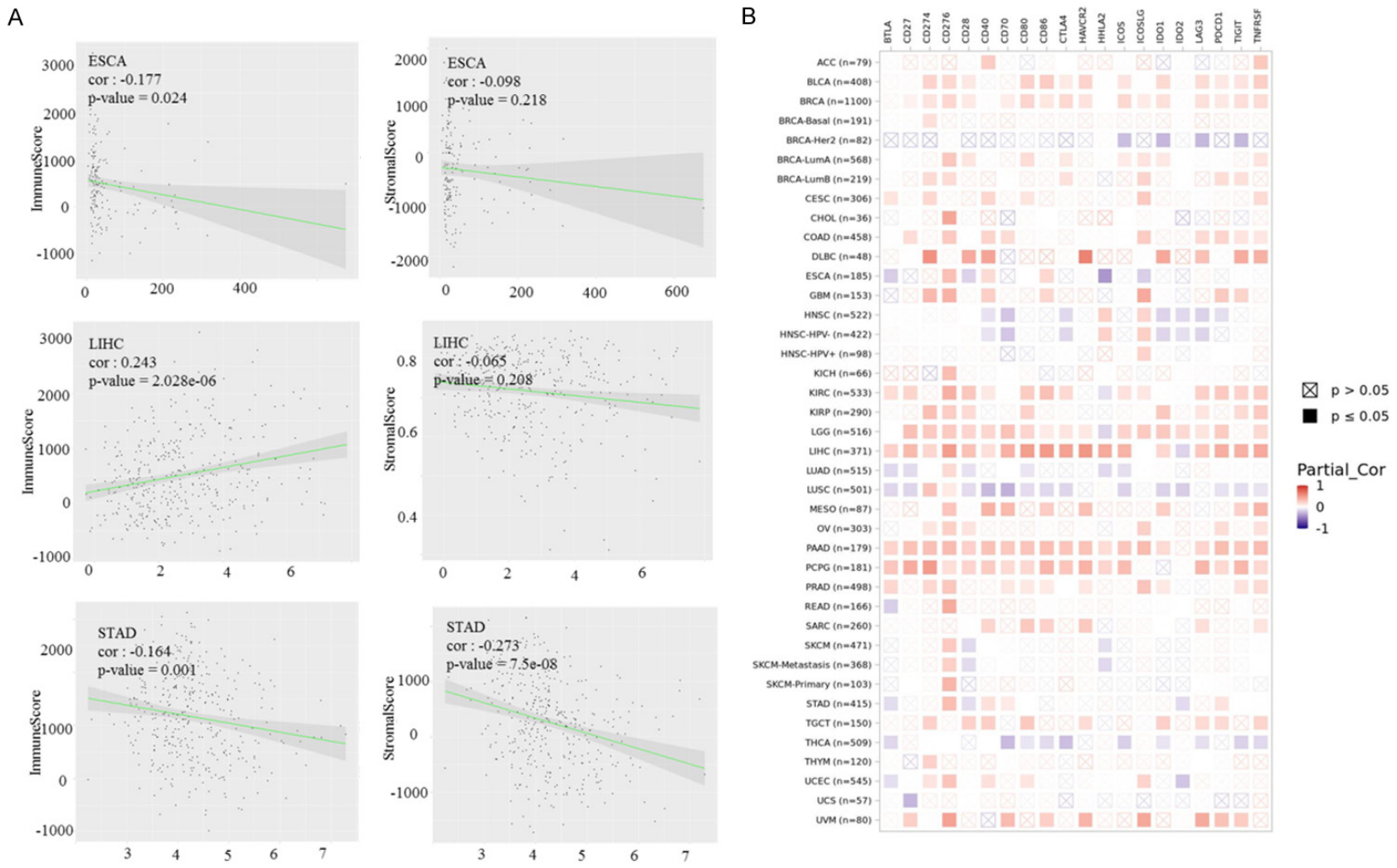
A
ESCA
cor : -0.177
p-value = 0.024
ESCA
cor : -0.098
p-value = 0.218
LIHC
cor : 0.243
p-value = 2.028e-06
LIHC
cor : -0.065
p-value = 0.208
STAD
cor : -0.164
p-value = 0.001
STAD
cor : -0.273
p-value = 7.5e-08
ImmuneScore
StromalScore
B
BTLA
CD27
CD274
CD276
CD28
CD40
CD70
CD80
CD86
CTLA4
HAVCR2
HHLA2
ICOS
ICOSLG
IDO1
IDO2
LAG3
PDCD1
TIGIT
TNFRSF
ACC (n=79)
BLCA (n=408)
BRCA (n=1100)
BRCA-Basal (n=191)
BRCA-Her2 (n=82)
BRCA-LumA (n=568)
BRCA-LumB (n=219)
CESC (n=306)
CHOL (n=36)
COAD (n=458)
DLBC (n=48)
ESCA (n=185)
GBM (n=153)
HNSC (n=522)
HNSC-HPV- (n=422)
HNSC-HPV+ (n=98)
KICH (n=66)
KIRC (n=533)
KIRP (n=290)
LGG (n=516)
LIHC (n=371)
LUAD (n=515)
LUSC (n=501)
MESO (n=87)
OV (n=303)
PAAD (n=179)
PCPG (n=181)
PRAD (n=498)
READ (n=166)
SARC (n=260)
SKCM (n=471)
SKCM-Metastasis (n=368)
SKCM-Primary (n=103)
STAD (n=415)
TGCT (n=150)
THCA (n=509)
THYM (n=120)
UCEC (n=545)
UCS (n=57)
UVM (n=80)
p > 0.05
p ≤ 0.05
Partial_Cor
1
0
-1

C

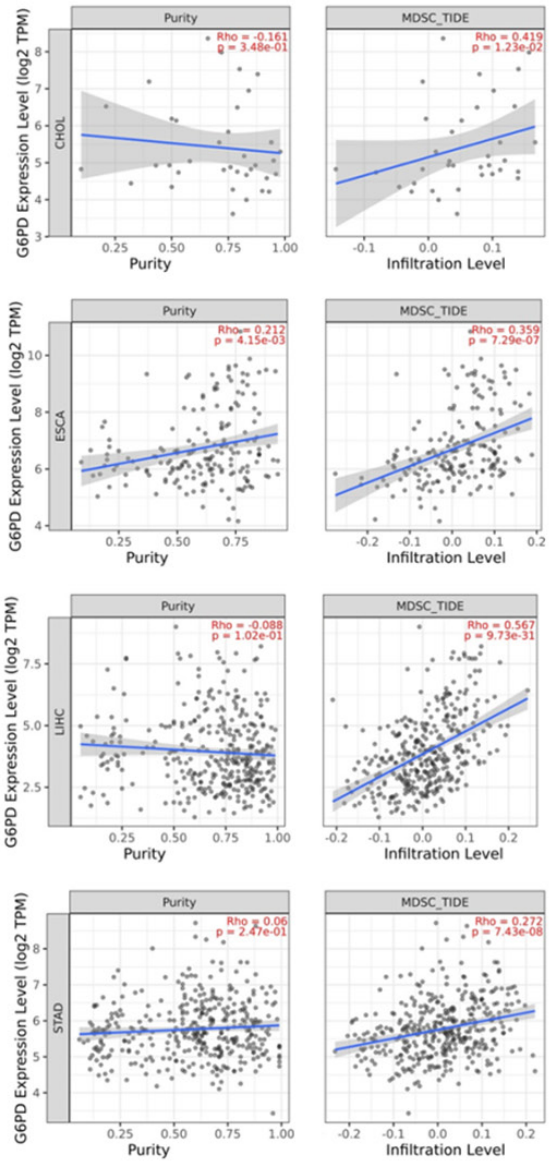
Purity
MDSC_TIDE
G6PD Expression Level (log2 TPM)
CHOL
Rho = -0.161
p = 3.48e-01
Rho = 0.419
p = 1.23e-02
ESCA
Rho = 0.212
p = 4.15e-03
Rho = 0.359
p = 7.29e-07
LIHC
Rho = -0.088
p = 1.02e-01
Rho = 0.567
p = 9.73e-31
STAD
Rho = 0.06
p = 2.47e-01
Rho = 0.272
p = 7.43e-08
Purity
Infiltration Level

D

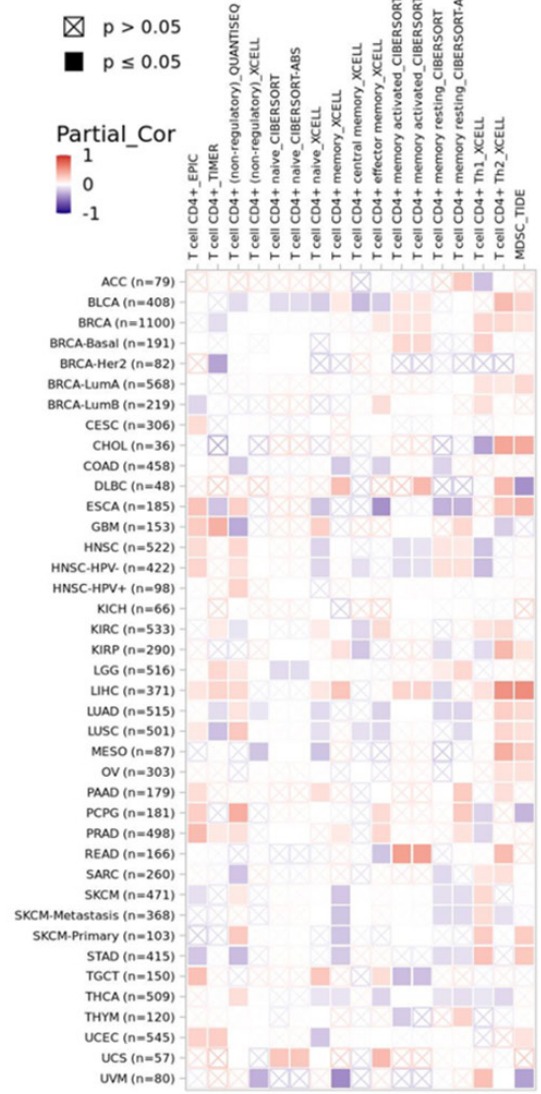
p > 0.05
p ≤ 0.05
Partial_Cor
1
0
-1
T cell CD4+_EPIC
T cell CD4+_TIMER
T cell CD4+ (non-regulatory)_QUANTISEQ
T cell CD4+ (non-regulatory)_XCELL
T cell CD4+ naive_CIBERSORT
T cell CD4+ naive_CIBERSORT-ABS
T cell CD4+ naive_XCELL
T cell CD4+ memory_XCELL
T cell CD4+ central memory_XCELL
T cell CD4+ effector memory_XCELL
T cell CD4+ memory activated_CIBERSORT
T cell CD4+ memory activated_CIBERSORT-ABS
T cell CD4+ memory resting_CIBERSORT
T cell CD4+ memory resting_CIBERSORT-ABS
T cell CD4+ Th1_XCELL
T cell CD4+ Th2_XCELL
MDSC_TIDE
ACC (n=79)
BLCA (n=408)
BRCA (n=1100)
BRCA-Basal (n=191)
BRCA-Her2 (n=82)
BRCA-LumA (n=568)
BRCA-LumB (n=219)
CESC (n=306)
CHOL (n=36)
COAD (n=458)
DLBC (n=48)
ESCA (n=185)
GBM (n=153)
HNSC (n=522)
HNSC-HPV- (n=422)
HNSC-HPV+ (n=98)
KICH (n=66)
KIRC (n=533)
KIRP (n=290)
LGG (n=516)
LIHC (n=371)
LUAD (n=515)
LUSC (n=501)
MESO (n=87)
OV (n=303)
PAAD (n=179)
PCPG (n=181)
PRAD (n=498)
READ (n=166)
SARC (n=260)
SKCM (n=471)
SKCM-Metastasis (n=368)
SKCM-Primary (n=103)
STAD (n=415)
TGCT (n=150)
THCA (n=509)
THYM (n=120)
UCEC (n=545)
UCS (n=57)
UVM (n=80)

Figure 10. Glucose 6 phosphatase dehydrogenase (G6PD) expression correlates with the immune infiltrates of tumors. (A) Top three scatter plots of correlation between G6PD expression and immune and stromal scores in multiple cancers. (B) Correlation between G6PD expression level and immune checkpoint-associated genes. (C) Correlations between G6PD expression level and the infiltration level of Myeloid derived suppressor cells (MDSCs), T helper cells (Th1) and Th2 subsets of CD4+ T cells across The Cancer Genome Atlas Program (TCGA) cancers. Scatter plots of MDSC (D) and CD4+ Th2 cell.

rimidine metabolism, mitosis, and steroid biosynthesis pathway.

Discussion

Gastrointestinal cancers are among the top 10 most prevalent and deadliest tumors worldwide. Gastrointestinal cancers includes ESCA, STAD, LIHC, COAD, CHOL, READ and PAAD. G6PD is known to be dysregulated in a variety of tumors, such as BRCA [31], LIHC [32] and ESCA [33]. However, whether G6PD is essential for tumor initiation, growth or metastasis remains unclear. In this study, we explored the panoncogene expression profile of G6PD. It was found that the expression of G6PD in gastrointestinal cancers is generally higher than that in normal tissues, which has broad research prospects. G6PD is conventionally considered as the first and rate-limiting enzyme of the PPP [34]. PPP produces large quantities of NADPH and ribose 5-phosphate for various cellular synthetic functions, such as the synthesis of aliphatic acid and sterols [10, 11]. In addition, this pathway ensures glutathione reduction, which enhances antioxidant defense and promotes cell proliferation [12]. These results reveal G6PD as a carcinogenic indicator of gastrointestinal cancers.

We studied the correlation between G6PD and the clinical features of gastrointestinal tumors, and found that G6PD functioned significantly on different classified groups with clinical features. Results revealed the expression of G6PD in Asians was the highest in CHOL, COAD and READ. As for ESCA, LIHC PAAD and STAD, the expression of G6PD was the highest in African American patients. G6PD expressed the highest in gastrointestinal cancer patients aged 41-60 years among all age levels. G6PD expressed higher in other groups than the Normal group in weight, stage, nodal metastasis and pathological stages. As for grade, it was seen that the higher the grade was, the higher expression of G6PD might be. ROC curves suggested that G6PD expression was associated with the diagnosis in gastrointestinal cancers based on TCGA and GEO database. G6PD showed an excellent predictive diagnosis ability particularly for LIHC, COAD, ESCA. KM survival curves indicated G6PD expression was correlated to the DFS of gastrointestinal cancer patients. G6PD up-regulated DFS in EAC and PAAD, and conversely in LIHC and STAD. Univariate Cox regression and stepwise multiple Cox regression analysis in R language both determined that G6PD expression was closely related with LIHC. Therefore, our study identified G6PD as a novel diagnosis marker of gastrointestinal cancers.

DNA structural changes could cause proto-oncogene mutations including point mutations, chromosome translocation, insertional mutagenesis, gene deletion and gene amplification [35]. We found that G6PD has a high mutation rate in COAD and ESCA. G6PD gene amplification was evident in ESCA, CHOL, PAAD and LIHC. G6PD copy number loss was found in LIHC. The expression of G6PD was even related to the mutation of TP53. G6PD level in COAD, ESCA, LIHC, PAAD, READ, and STAD patients with TP53 mutation was higher than that in patients without TP53 mutation. It can be seen that the abnormality of G6PD gene may be related to the development of gastrointestinal cancers. We studied the correlation of G6PD with TMB and MSI in gastrointestinal tumors, and the correlation of G6PD with immune score and matrix score. The results showed that the absolute values were all below 0.4.

Multifactorial drug resistance is regarded as the major cause of treatment failure in gastrointestinal cancers. Accumulating evidence has shown that the constituents of TME, including cancer-associated fibroblasts, tumor vasculature, immune cells, physical factors, cytokines and exosomes may explain the therapeutic resistance mechanisms in gastrointestinal cancers [36]. Recent studies have confirmed improvement in advanced cancer treatment by new immunocheckpoint inhibitors and antibody drug conjugates [37]. However, only a few numbers of patients with specific types of cancers

Gastrointestinal cancers

Figure 11. Drug Sensitivity Analysis of Glucose 6 phosphatase dehydrogenase (G6PD) related gene sets: G6PD, B and T lymphocyte associated (BTLA), Cluster of differentiation 27 (CD27), CD274 and CD276 in GSCALite database.

respond to immunotherapy, which may be due to insufficient immune activation and failure to recognize tumor specific antigens [38]. Therefore, identifying other potential therapeutic targets and determining the correlation between potential genes and current immune checkpoints are of great value for tumor immunotherapy. In this study, G6PD level was shown to have positive or negative correlation with multiple immune checkpoint molecules in gastrointestinal cancers. Especially, G6PD was positively correlated with CD276 in all gastrointestinal cancers, and negatively with HHLA2 in ESCA and STAD. It can be seen that G6PD may be of great significance in exploring new treatments of gastrointestinal cancers.

A large amount of evidence supports that immune cells are very important in immune response under pathological conditions, and play an important role in angiogenesis and metastasis in tumor growth [39]. Immune cells are known to have an ability to mediate the destruction of cancer cells and to influence the microenvironment of tumors, leading to the suppression or progression of tumor growth. The expression of key genes involved in immune response and regulation can provide crucial information about the immune status of tumors and the potential efficacy of immunotherapy. G6PD, as a well-known enzyme involved in metabolic processes, has recently been recognized for its potential role in regulating immune function in the context of cancer. Our findings suggest that G6PD expression is associated with the proportion of immune and stromal cells in the TME, and it is correlated with the expression of immune checkpoint genes and immune cell infiltration in various cancers.

Taken together, these results highlight the importance of further investigating the role of G6PD in regulating the immune response and its potential as a therapeutic target in cancer treatment. CD4+ T cell subsets (Th1, Th2, Th17 and regulatory T (Treg) cells) play an important role in this process. For example, the Th2 subgroup can secrete cytokines IL-4, IL-5 and IL-13, activate B cells into plasma cells, and secrete antibodies [40]. Our study showed that the abnormal expression of G6PD was due to the increase of T cell CD4+ Th2 subsets and decrease of T cell CD4+ cells (non-regulatory). We searched G6PD related gene sets, including “immune genes” BTLA, CD27, CD274, CD276 to perform drug sensitivity analysis. G6PD was found to be sensitive to FK866, Phenformin, AICAR etc., while resistant to RO-3306, CGP-082996, TGX221 etc. All these indicate the potential clinical application value of G6PD in immunotherapy of gastrointestinal cancers, which needs further verification.

In terms of G6PD associated proteins and signal pathways, we found that G6PD interacted closely with PGD, HK2, LDHB, TPI1, GPI, PKM, PGLS, TALDO1, GAPDH and TP53, among which TP53 was closely related to tumors. G6PD was related to aging, nutritional response, daunorubicin metabolism, doxorubicin metabolism, prostaglandin metabolism and other biological processes related to tumor growth, chemotherapy resistance, tumor pain, etc. G6PD is related to pentose PPP, cytochrome P450 metabolism of exogenous substances, glutathione metabolism, iron poisoning, chemical carcinogenic reactive oxygen species and other signal pathways closely related to cancers. We used the Cancer SEA database for single cell analysis, and found that G6PD was involved in a variety of carcinogenic processes, including angiogenesis, apoptosis, cell cycle differentiation, DNA damage, DNA pairing, EMT, etc.

The oxidative branch of PPP mainly produces NADPH and R5P [41]. NADPH can not only maintain the redox state, but also is the main molecule of lipid and nucleotide synthesis [42, 43]. Among them, the key enzyme of oxidative branch is G6PD. These pathways can effect oxidative metabolism in gastrointestinal tumors through G6PD. Due to the heterogeneity of tumor metabolism, the high PPP flow of tumor cells is different from that of normal cells [44-46]. At the same time, NADPH is used to maintain the balance of intracellular redox reactions. This study reports on the close correlation of G6PD with gastrointestinal cancers, to provide further theoretical basis for clinical treatment-related research, such as tumor anti-metabolism therapy, and gives references for subsequent experimental verification.

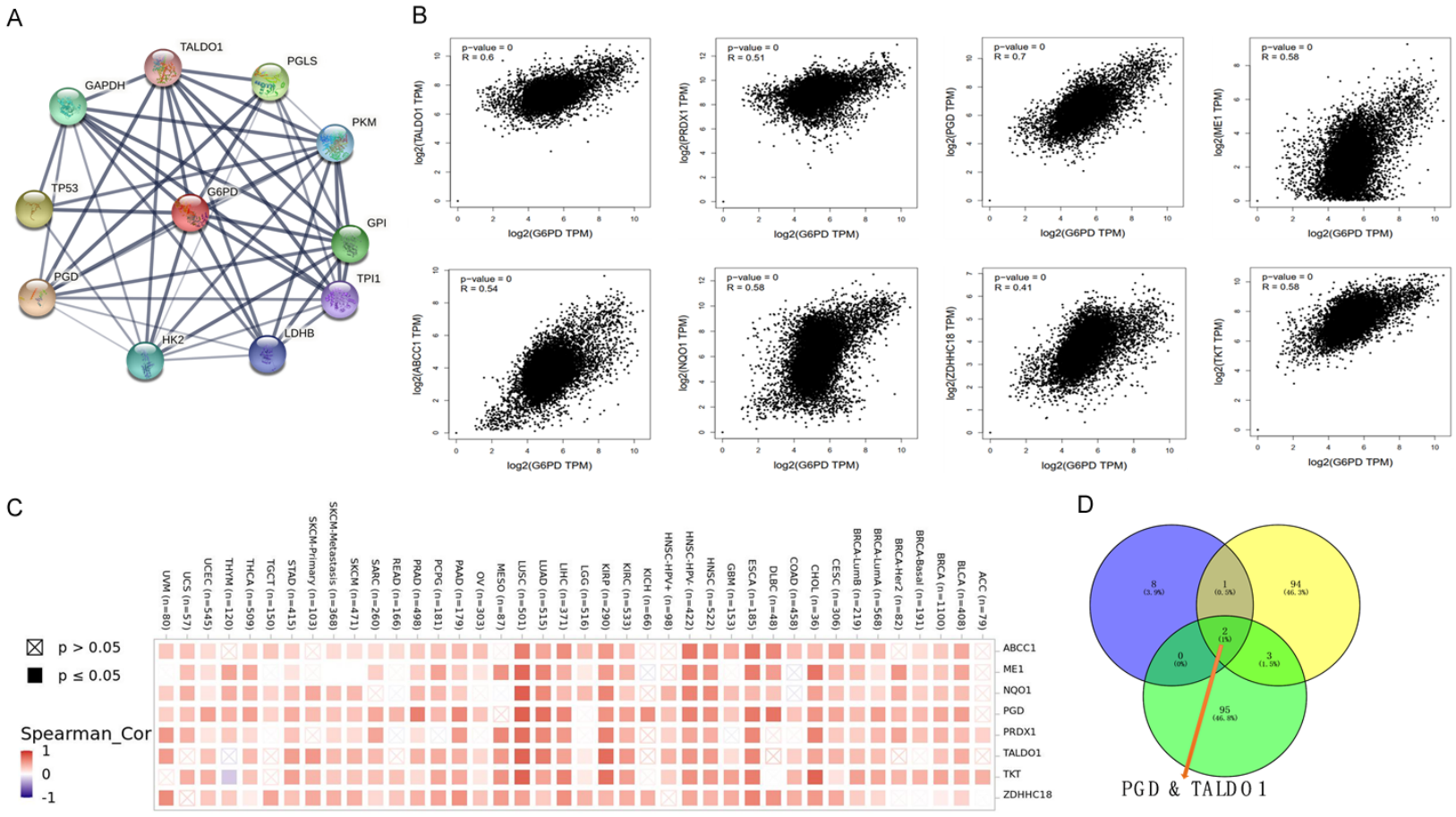
A
TALDO1
PGLS
GAPDH
PKM
TP53
G6PD
GPI
PGD
TPI1
HK2
LDHB
B
p-value = 0
R = 0.6
log2(TALDO1 TPM)
log2(G6PD TPM)
p-value = 0
R = 0.51
log2(PRDX1 TPM)
log2(G6PD TPM)
p-value = 0
R = 0.7
log2(PGD TPM)
log2(G6PD TPM)
p-value = 0
R = 0.58
log2(ME1 TPM)
log2(G6PD TPM)
p-value = 0
R = 0.54
log2(ABCC1 TPM)
log2(G6PD TPM)
p-value = 0
R = 0.58
log2(NQO1 TPM)
log2(G6PD TPM)
p-value = 0
R = 0.41
log2(ZDHHC18 TPM)
log2(G6PD TPM)
p-value = 0
R = 0.58
log2(TKT TPM)
log2(G6PD TPM)
C
p > 0.05
p ≤ 0.05
Spearman_Cor
1
0
-1
UVM (n=80)
UCS (n=57)
UCEC (n=545)
THYM (n=120)
THCA (n=509)
TGCT (n=150)
STAD (n=415)
SKCM-Primary (n=103)
SKCM-Metastasis (n=368)
SKCM (n=471)
SARC (n=260)
READ (n=166)
PRAD (n=498)
PCPG (n=181)
PAAD (n=179)
OV (n=303)
MESO (n=87)
LUSC (n=501)
LUAD (n=515)
LIHC (n=371)
LGG (n=516)
KIRP (n=290)
KIRC (n=533)
KICH (n=66)
HNSC-HPV+ (n=98)
HNSC-HPV- (n=422)
HNSC (n=522)
GBM (n=153)
ESCA (n=185)
DLBC (n=48)
COAD (n=458)
CHOL (n=36)
CESC (n=306)
BRCA-LumB (n=219)
BRCA-LumA (n=568)
BRCA-Her2 (n=82)
BRCA-Basal (n=191)
BRCA (n=1100)
BLCA (n=408)
ACC (n=79)
ABCC1
ME1
NQO1
PGD
PRDX1
TALDO1
TKT
ZDHHC18
D
8
(3.9%)
1
(0.5%)
94
(46.3%)
2
(1%)
0
(0%)
3
(1.5%)
95
(46.8%)
PGD & TALDO1

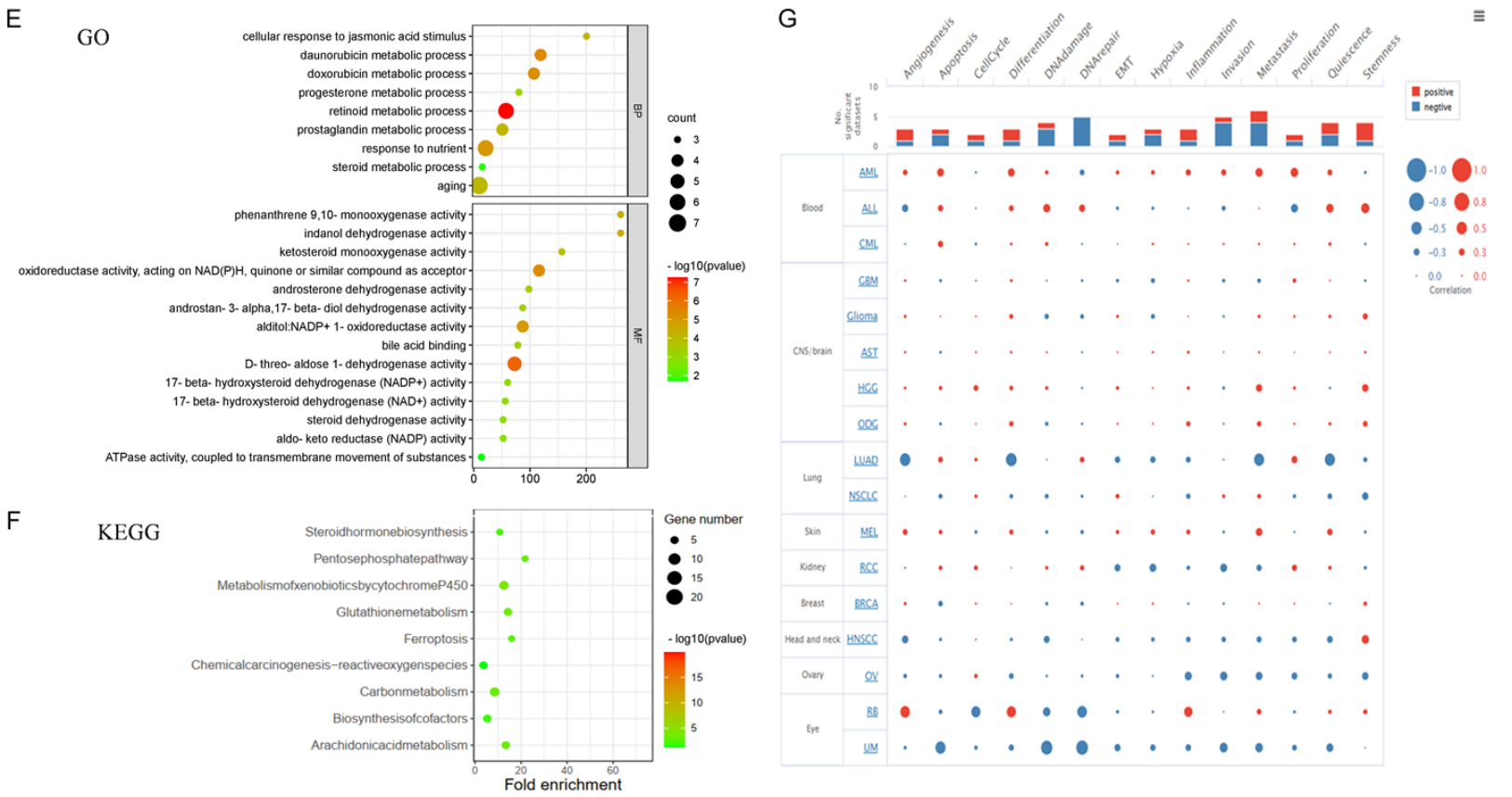

Figure 12. Enrichment analysis of Glucose 6 phosphatase dehydrogenase (G6PD)-related partners. (A) Protein-protein interaction (PPI) network for G6PD was constructed in Cytoscape. (B) The correlation between G6PD expression and selected targeting genes, including Transaldolase 1 (TALDO1), Peroxiredoxin 1 (PRDX1), phosphogluconate dehydrogenase (PGD), Malatase 1 (ME1), ATP binding cassette subfamily C member 1 (ABCC1), NAD(P)H Quinone Dehydrogenase 1 (NQO1), Zinc Finger DHHC-Type Palmitoyltransferase 18 (ZDHHC18) and Transketolase (TKT). (C) The heatmap showed that G6PD was positively related to the selected genes in The Cancer Genome Atlas program (TCGA) cancers. (D) Venn diagram of G6PD-interacted and correlated genes. Gene Ontology (GO) Biological Process and molecular function (E) Kyoto Encyclopedia of Genes and Genomes (KEGG) pathway (F) enrichment analyses were performed. (G) CancerSEA was utilized for single-cell analysis to determine the functions of G6PD.

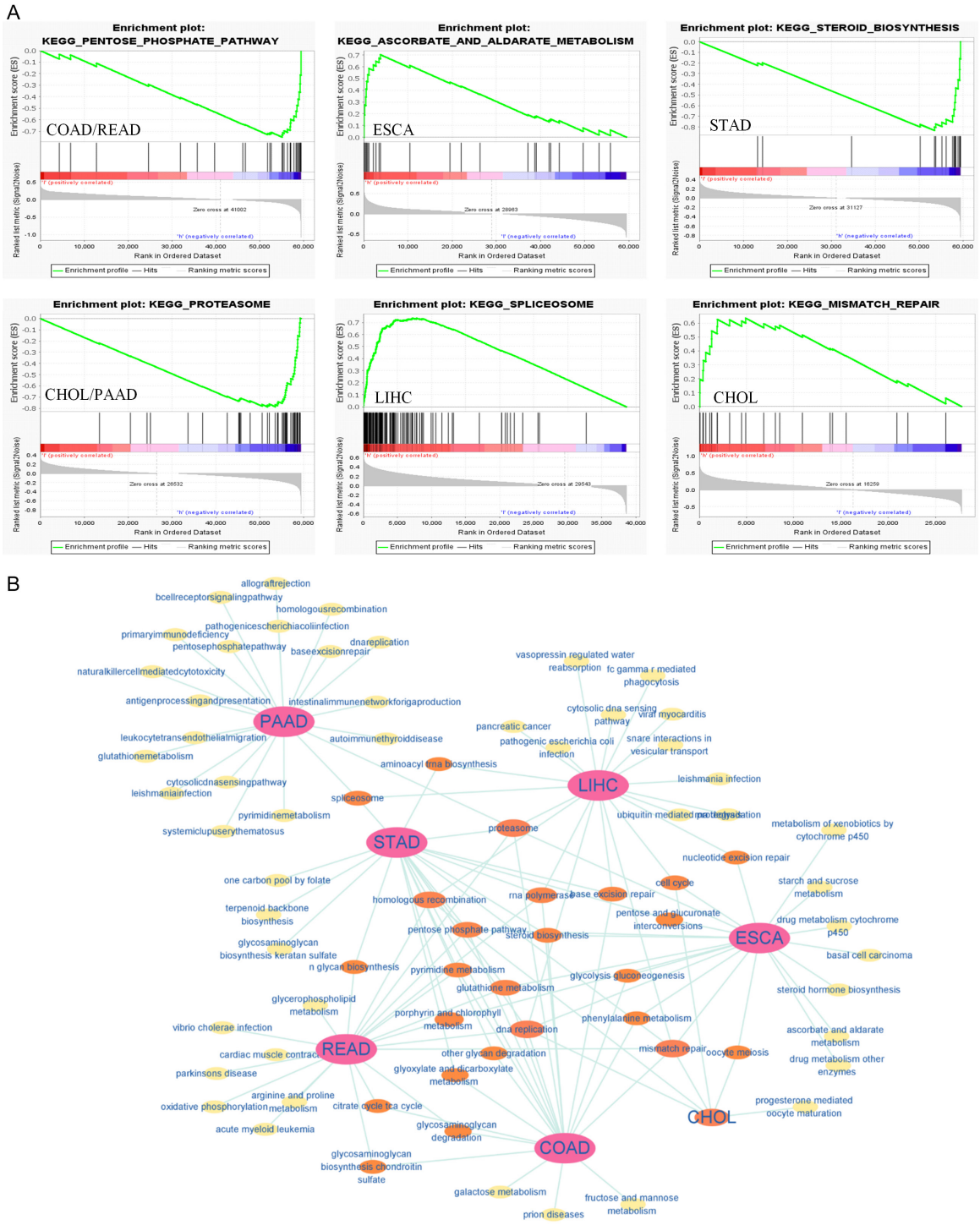

Figure 13. Enrichment analysis of Glucose 6 phosphatase dehydrogenase (G6PD)-related partners. A. Sorting according to ES score shows the signal path with the best ES score. B. Network diagram of different cancer signaling pathways.

In a word, G6PD is likely to promote gastrointestinal cancers through the above mechanism, and these views are worthy of verification in subsequent experiments.

Acknowledgements

Special project of high-level talent scientific research project in the affiliated Hospital of

Youjiang Medical College for nationalities in 2020. Project name: mechanism of MiR-483-5p targeted enhancer-mediated upregulation of IGF2 and H19 gene expression in hepatocellular carcinoma cells contract number: R202011703.

Disclosure of conflict of interest

None.

Address correspondence to: Tong-Hua Wang, Department of Gastroenterology, The Affiliated Hospital of Youjiang Medical University for Nationalities, Baise 533000, Guangxi, China. Tel: +86-0776-2825103; E-mail: 67919054@qq.com

References

[1] Xu Z, Zeng S, Gong Z and Yan Y. Exosome-based immunotherapy: a promising approach for cancer treatment. Mol Cancer 2020; 19: 160.

[2] Siegel RL, Miller KD, Wagle NS and Jemal A. Cancer statistics, 2023. CA Cancer J Clin 2023; 73: 17-48.

[3] Manzella G, Schreck LD, Breunis WB, Molenaar J, Merks H, Barr FG, Sun W, Rommele M, Zhang L, Tchinda J, Ngo QA, Bode P, Delattre O, Surdez D, Rekhi B, Niggli FK, Schafer BW and Wachtel M. Phenotypic profiling with a living biobank of primary rhabdomyosarcoma unravels disease heterogeneity and AKT sensitivity. Nat Commun 2020; 11: 4629.

[4] Duffy MJ. Tumor markers in clinical practice: a review focusing on common solid cancers. Med Princ Pract 2013; 22: 4-11.

[5] International Human Genome Sequencing Consortium. Finishing the euchromatic sequence of the human genome. Nature 2004; 431: 931-945.

[6] Wang Z, Gerstein M and Snyder M. RNA-Seq: a revolutionary tool for transcriptomics. Nat Rev Genet 2009; 10: 57-63.

[7] Ma H, Zhang F, Zhou L, Cao T, Sun D, Wen S, Zhu J, Xiong Z, Tsau MT, Cheng ML, Hung LM, Zhou Y and Li Q. c-Src facilitates tumorigenesis by phosphorylating and activating G6PD. Oncogene 2021; 40: 2567-2580.

[8] Meng Q, Zhang Y, Hao S, Sun H, Liu B, Zhou H, Wang Y and Xu ZX. Recent findings in the regulation of G6PD and its role in diseases. Front Pharmacol 2022; 13: 932154.

[9] Luzzatto L and Arese P. Favism and glucose-6-phosphate dehydrogenase deficiency. N Engl J Med 2018; 378: 60-71.

[10] Tang BL. Neuroprotection by glucose-6-phosphate dehydrogenase and the pentose phosphate pathway. J Cell Biochem 2019; 120: 14285-14295.

[11] Lu M, Lu L, Dong Q, Yu G, Chen J, Qin L, Wang L, Zhu W and Jia H. Elevated G6PD expression contributes to migration and invasion of hepatocellular carcinoma cells by inducing epithelial-mesenchymal transition. Acta Biochim Biophys Sin (Shanghai) 2018; 50: 370-380.

[12] Yang HC, Wu YH, Liu HY, Stern A and Chiu DT. What has passed is prolog: new cellular and physiological roles of G6PD. Free Radic Res 2016; 50: 1047-1064.

[13] Luzzatto L and Seneca E. G6PD deficiency: a classic example of pharmacogenetics with on-going clinical implications. Br J Haematol 2014; 164: 469-480.

[14] Longo L, Vanegas OC, Patel M, Rosti V, Li H, Waka J, Merghoub T, Pandolfi PP, Notaro R, Manova K and Luzzatto L. Maternally transmitted severe glucose 6-phosphate dehydrogenase deficiency is an embryonic lethal. EMBO J 2002; 21: 4229-4239.

[15] Sun L, Suo C, Li ST, Zhang H and Gao P. Metabolic reprogramming for cancer cells and their microenvironment: beyond the Warburg effect. Biochim Biophys Acta Rev Cancer 2018; 1870: 51-66.

[16] Jiang P, Du W, Wang X, Mancuso A, Gao X, Wu M and Yang X. p53 regulates biosynthesis through direct inactivation of glucose-6-phosphate dehydrogenase. Nat Cell Biol 2011; 13: 310-316.

[17] Li R, Wang W, Yang Y and Gu C. Exploring the role of glucose-6-phosphate dehydrogenase in cancer (Review). Oncol Rep 2020; 44: 2325-2336.

[18] Barajas JM, Reyes R, Guerrero MJ, Jacob ST, Motiwala T and Ghoshal K. The role of miR-122 in the dysregulation of glucose-6-phosphate dehydrogenase (G6PD) expression in hepatocellular cancer. Sci Rep 2018; 8: 9105.

[19] Hong X, Song R, Song H, Zheng T, Wang J, Liang Y, Qi S, Lu Z, Song X, Jiang H, Liu L and Zhang Z. PTEN antagonises Tcl1/hnRNPK-mediated G6PD pre-mRNA splicing which contributes to hepatocarcinogenesis. Gut 2014; 63: 1635-1647.

[20] Liu Z, Chen Y, Wang L and Ji S. ALKBH5 promotes the proliferation of glioma cells via enhancing the mRNA stability of G6PD. Neurochem Res 2021; 46: 3003-3011.

[21] Li Z, He Y, Li Y, Li J, Zhao H, Song G, Miyagishi M, Wu S and Kasim V. NeuroD1 promotes tumor cell proliferation and tumorigenesis by directly activating the pentose phosphate pathway in colorectal carcinoma. Oncogene 2021; 40: 6736-6747.

[22] Su Z, Gao A, Li X, Zou S, He C, Wu J, Ding WQ and Zhou J. DNA polymerase IOTA promotes esophageal squamous cell carcinoma proliferation through Erk-OGT-induced G6PD overactivation. Front Oncol 2021; 11: 706337.

[23] Hu DG, Marri S, Hulin JA, McKinnon RA, Mackenzie PI and Meech R. The somatic mutation landscape of UDP-glycosyltransferase (UGT) genes in human cancers. Cancers (Basel) 2022; 14: 5708.
[24] Yoshihara K, Shahmoradgoli M, Martinez E, Vegesna R, Kim H, Torres-Garcia W, Trevino V, Shen H, Laird PW, Levine DA, Carter SL, Getz G, Stemke-Hale K, Mills GB and Verhaak RG. Inferring tumour purity and stromal and immune cell admixture from expression data. Nat Commun 2013; 4: 2612.
[25] Liang Z, Pan L, Shi J and Zhang L. C1QA, C1QB, and GZMB are novel prognostic biomarkers of skin cutaneous melanoma relating tumor microenvironment. Sci Rep 2022; 12: 20460.
[26] Wu A, Zhao C, Mou S, Li S, Cui X and Zhang R. Integrated analysis identifies the IL6/JAK/STAT signaling pathway and the estrogen response pathway associated with the pathogenesis of intracranial aneurysms. Front Immunol 2022; 13: 1046765.
[27] Zhao Y, Zhang M, Pu H, Guo S, Zhang S and Wang Y. Prognostic implications of pan-cancer CMTM6 expression and its relationship with the immune microenvironment. Front Oncol 2020; 10: 585961.
[28] Szklarczyk D, Gable AL, Lyon D, Junge A, Wyder S, Huerta-Cepas J, Simonovic M, Doncheva NT, Morris JH, Bork P, Jensen LJ and Mering CV. STRING v11: protein-protein association networks with increased coverage, supporting functional discovery in genome-wide experimental datasets. Nucleic Acids Res 2019; 47: D607-D613.
[29] Otasek D, Morris JH, Boucas J, Pico AR and Demchak B. Cytoscape automation: empowering workflow-based network analysis. Genome Biol 2019; 20: 185.
[30] Yuan H, Yan M, Zhang G, Liu W, Deng C, Liao G, Xu L, Luo T, Yan H, Long Z, Shi A, Zhao T, Xiao Y and Li X. CancerSEA: a cancer single-cell state atlas. Nucleic Acids Res 2019; 47: D900-D908.
[31] Jacquier V, Gitenay D, Cavailles V and Teyssier C. The transcription coregulator RIP140 inhibits cancer cell proliferation by targeting the pentose phosphate pathway. Int J Mol Sci 2022; 23: 7419.
[32] Zhang Y, Ren H, Zhang C, Li H, Guo Q, Xu H and Cui L. Development and validation of four ferroptosis-related gene signatures and their correlations with immune implication in hepatocellular carcinoma. Front Immunol 2022; 13: 1028054.
[33] Zhu L, Yang F, Wang L, Dong L, Huang Z, Wang G, Chen G and Li Q. Identification the ferroptosis-related gene signature in patients with esophageal adenocarcinoma. Cancer Cell Int 2021; 21: 124.
[34] Jiang A, Guo H, Jiang X, Tao J, Wu W and Liu H. G6PD deficiency is crucial for insulin signaling activation in skeletal muscle. Int J Mol Sci 2022; 23: 7425.
[35] Yang Z, Qi X, Gross N, Kou X, Bai Y, Feng Y, Wang B, Zafereo ME, Li G, Sun C, Li H, Chen X and Huang Z. The synergy of germline C634Y and V292M RET mutations in a northern Chinese family with multiple endocrine neoplasia type 2A. J Cell Mol Med 2020; 24: 13163-13170.
[36] Zhang J, Han H, Wang L, Wang W, Yang M and Qin Y. Overcoming the therapeutic resistance of hepatomas by targeting the tumor microenvironment. Front Oncol 2022; 12: 988956.
[37] Xu Z, Ma J, Chen T and Yang Y. Case report: the remarkable response of pembrolizumab combined with RC48 in the third-line treatment of metastatic urothelial carcinoma. Front Immunol 2022; 13: 978266.
[38] Lv M, Chen M, Zhang R, Zhang W, Wang C, Zhang Y, Wei X, Guan Y, Liu J, Feng K, Jing M, Wang X, Liu YC, Mei Q, Han W and Jiang Z. Manganese is critical for antitumor immune responses via cGAS-STING and improves the efficacy of clinical immunotherapy. Cell Res 2020; 30: 966-979.
[39] Gabrilovich DI. Myeloid-derived suppressor cells. Cancer Immunol Res 2017; 5: 3-8.
[40] Li Q, Zou J, Wang M, Ding X, Chepelev I, Zhou X, Zhao W, Wei G, Cui J, Zhao K, Wang HY and Wang RF. Critical role of histone demethylase Jmjd3 in the regulation of CD4+ T-cell differentiation. Nat Commun 2014; 5: 5780.
[41] Vaupel P, Schmidberger H and Mayer A. The Warburg effect: essential part of metabolic reprogramming and central contributor to cancer progression. Int J Radiat Biol 2019; 95: 912-919.
[42] Ge T, Yang J, Zhou S, Wang Y, Li Y and Tong X. The role of the pentose phosphate pathway in diabetes and cancer. Front Endocrinol (Lausanne) 2020; 11: 365.
[43] Hayes JD, Dinkova-Kostova AT and Tew KD. Oxidative stress in cancer. Cancer Cell 2020; 38: 167-197.
[44] Farhadi P, Yarani R, Dokaneheifard S and Mansouri K. The emerging role of targeting cancer metabolism for cancer therapy. Tumour Biol 2020; 42: 1010428320965284.
[45] Saikolappan S, Kumar B, Shishodia G, Koul S and Koul HK. Reactive oxygen species and cancer: a complex interaction. Cancer Lett 2019; 452: 132-143.
[46] Peltonen R, Ahopelto K, Hagstrom J, Bockelman C, Haglund C and Isoniemi H. High TKTL1 expression as a sign of poor prognosis in colorectal cancer with synchronous rather than metachronous liver metastases. Cancer Biol Ther 2020; 21: 826-831.